

1 **Title:** *Seeing herbaria in a new light*: leaf reflectance spectroscopy unlocks
2 predictive trait and classification modeling in plant biodiversity collections

3 **Authors:** Dawson M. White^{1,2*}, Jeannine Cavender-Bares^{1,2,*}, Charles C. Davis^{1,2}, J. Antonio Guzmán
4 Q.^{1,2}, Shan Kothari³, Jorge M. Robles⁴, Jose Eduardo Meireles⁵

5 Authors for correspondence: Dawson M. White, dawson.white@gmail.com; Jeannine Cavender-Bares,
6 jcavender@fas.harvard.edu

7 **Affiliations:**

8 ¹Harvard University Herbaria, 22 Divinity Ave., Cambridge, MA 02138 USA

9 ²Department of Organismic and Evolutionary Biology, Harvard University, Cambridge, MA 02138 USA

10 ³Department of Renewable Resources, University of Alberta, Canada

11 ⁴Department of Biological Sciences, California State University San Marcos, San Marcos, CA 92078
12 USA

13 ⁵School of Biology and Ecology and University of Maine Herbarium, University of Maine, 5735 Hitchner
14 Hall, Orono, ME 04469 USA.

15
16 **Summary:**

- 17 • Reflectance spectroscopy is a non-destructive, rapid, and robust method for estimating functional
18 traits and distinguishing species. Spectral reflectance libraries generated from herbarium
19 specimens are an untapped and promising resource for generating broad phenomic datasets across
20 space, time, and species.
- 21 • We conducted a proof-of-concept study using functional trait data and spectra from recently
22 dried, pressed leaves, alongside data from herbarium specimens up to 179 years old. We assessed
23 the utility and transferability of these datasets for functional trait prediction and taxonomic
24 discrimination.
- 25 • Herbarium spectra discriminated species with 74% accuracy and predicted leaf mass per area
26 (LMA) with $R^2=0.92$ and %RMSE=5.8%. Models for LMA prediction were transferable between
27 herbarium and pressed spectra, achieving $R^2=0.88$, %RMSE=8.76% for herbarium to pressed
28 spectra, and $R^2=0.76$, %RMSE=10.5% for the reverse transfer.
- 29 • The results demonstrate the feasibility of using herbarium spectral data for functional trait
30 prediction and taxonomic discrimination. This success provides methodological guidance for
31 advancing the global Metaherbarium and integrating spectral reflectance into next-generation
32 digitization efforts for plant biodiversity collections.

33

34 **Plain language summary:** Reflectance spectroscopy applied to herbarium collections offers a
35 transformative method to generate phenomic data across the plant tree of life. Despite preservation
36 challenges, we demonstrate its reliability in predicting functional traits and facilitating taxonomic
37 discrimination in specimens with a median age of 91 years. We further provide guidelines for researchers
38 and collections managers to collect and scale spectra effectively.

39 Introduction

40 The vision of herbarium spectral scanning

41 The urgency of global biodiversity assessment is driving the application of reflectance spectroscopy as a
42 broadly informative technology for advancing systematic knowledge of plant diversity at scales ranging
43 from molecules to continents (Serbin *et al.*, 2014; Cavender-Bares *et al.*, 2017, In Review.; Meireles *et*
44 *al.*, 2020). This powerful approach provides a rapid and non-destructive method to characterize leaf
45 functional traits and identify taxa through spectral signals, integrating structural, chemical, and
46 physiological information from plants in various contexts, including the lab, herbarium, and field (Box 1;
47 Costa *et al.*, 2018; Serbin & Townsend, 2020; Kothari & Schweiger, 2022). Despite its potential, the
48 spectral-based taxonomic and functional characterization of plant diversity faces significant challenges.
49 Limited access to material from remote geographic regions and uncommon taxa results in spectral
50 datasets that are both biased and highly sparse (Meireles *et al.*, 2020), even more so than global plant trait
51 databases (Jetz *et al.*, 2016). Addressing this limitation requires extensive, costly, and time-intensive
52 fieldwork. Additionally, the lack of linkage between leaf spectral data and voucher specimens undermines
53 geographic and temporal precision and compromises reliability as inevitable taxonomic and
54 nomenclatural changes occur.

55 A promising path forward for filling these gaps across the plant tree of life lies in leveraging the
56 approximately 400 million dried plant specimens stored in over 3,500 herbaria worldwide (Thiers, 2020;
57 Heberling, 2022; Kothari *et al.*, 2023). Herbarium collections are the physical foundation of our scientific
58 understanding of plant and fungal diversity and anchor every species definition. Herbarium collections
59 also include specimens that are rare, extinct, or regionally extirpated. By grounding plant taxonomy and
60 spatial data with diverse extended datasets, the wealth of global herbarium specimens have long been a
61 key resource for researchers studying plant diversity and ecological and evolutionary processes across
62 spatial and temporal scales (Davis, 2023).

63 The integration of reflectance spectroscopy into herbarium digitization pipelines, with appropriate
64 and standardized modifications, would result in the rapid generation of spectral data directly linked to
65 physical specimens. This would create a new dimension of phenomic data integrated with other extended
66 specimen datasets and tremendously improve capacities for taxonomic, ecological, and evolutionary
67 investigations. Integrating spectral data with herbarium specimens would not only expand trait datasets
68 but also deepen our understanding of plant functional diversity across space and time.

69 However, until now, the promise of this innovative use of herbarium reflectance spectroscopy is
70 tempered by the reality that we have yet to empirically prove the utility of herbarium specimens, given the
71 potential for tissue degradation with mounting, preservation, and storage. Spectral scans with modern

72 spectroradiometers (350–2,500 nm) are highly sensitive to all physical aspects of scanned materials and
73 require rigorous standardized protocols in the field and laboratory to ensure high data quality and
74 aggregation from different sources and sensors. Herbarium specimens present unique challenges given the
75 extra variables beyond the normal biological variation that has affected their tissues (Fig. 2).
76

Box 1: Learning from spectra

Reflectance spectroscopy measures light reflected from a material — typically from the visible, near-infrared, and short-wave infrared wavelengths (350–2,500 nm) — across hundreds of specific wavelength bands (Fig. 1). These scans reveal absorption features associated with the structural and chemical properties of the target material, such as leaf tissue (Curran, 1989). Spectral scans are fast (two to three seconds), require minimal digital resources (30–40 KB per file), and enable powerful predictive modeling using chemometric and machine-learning approaches such as partial least squares regression, discriminant analysis, and neural networks.

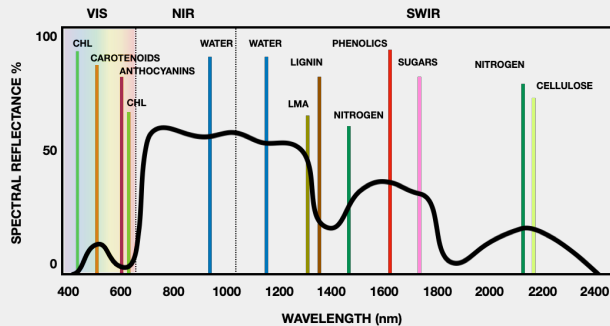


Fig. 1. Typical fresh leaf spectrum showing the percentage of light reflected across the visible (VIS), Near-Infrared (NIR) and Short-Wave Infrared light regions and highlighting a few absorption features associated with leaf chemistry and structure. Redrawn from Cavender-Bares *et al.*, in review.

Spectra have been widely used to predict leaf functional traits — such as leaf mass per area (LMA) and leaf nitrogen content — that reveal plant resource use strategies and ecological roles, offering insights into species interactions, community assembly, and ecosystem functions such as productivity and disturbance resistance (Wright *et al.*, 2004; Díaz *et al.*, 2016). Estimating traits is critical for understanding biodiversity responses to global change, refining predictive models of ecosystem function, and monitoring plant strategies and resource availability across scales efficiently (Díaz *et al.*, 2016; Funk *et al.*, 2017).

Reflectance spectroscopy also offers a robust, non-destructive method for taxonomic classification by capturing the unique spectral profiles of different taxa (Meireles *et al.*, 2020), allowing researchers to distinguish species, populations, and even hybrids with accuracies comparable to genetic barcoding (72–100%; Abasolo *et al.*, 2013; Lang *et al.*, 2017; Stasinski *et al.*, 2021).

By integrating signals from leaf structural, chemical, and physiological traits, spectra facilitate species identification and offer insights into ecological and evolutionary processes (Cavender-Bares *et al.*, 2016, Cavender-Bares *et al.*, in review.; Cotrozzi *et al.*, 2017; Meireles *et al.*, 2020; Kothari & Schweiger, 2022).

Recent advances demonstrate that spectral data taken from both fresh and recently dried leaf samples can be effectively used to generate accurate predictive models for taxonomic discrimination and functional trait values (Durgante *et al.*, 2013; Costa *et al.*, 2018; Kothari *et al.*, 2023).

79 The plant tissues in herbaria have been altered by dynamic collection, processing, and
80 preservation techniques with variable storage conditions and durations, ranging from months to centuries.
81 Variability in preservation methods across institutions globally and over time have inevitably led to subtle
82 changes in tissue structure and composition that create challenges to aggregating and comparing data.
83 Preservation and pest removal have in many cases introduced contamination in the form of chemical
84 residues or post-mortem biological agents (Bieker *et al.*, 2020). There is also the problem that plant
85 specimens are glued to herbarium paper, and reflectance scans of glued portions of these specimens will
86 be mixed with the chemical components and structure of these materials (see Neto-Bradley *et al.*). As
87 herbaria are just beginning to incorporate spectral scanning into their digitization pipelines, there is
88 urgency in communicating the unique challenges of herbarium spectral scanning to establish standardized
89 protocols that ensure data quality and compatibility.

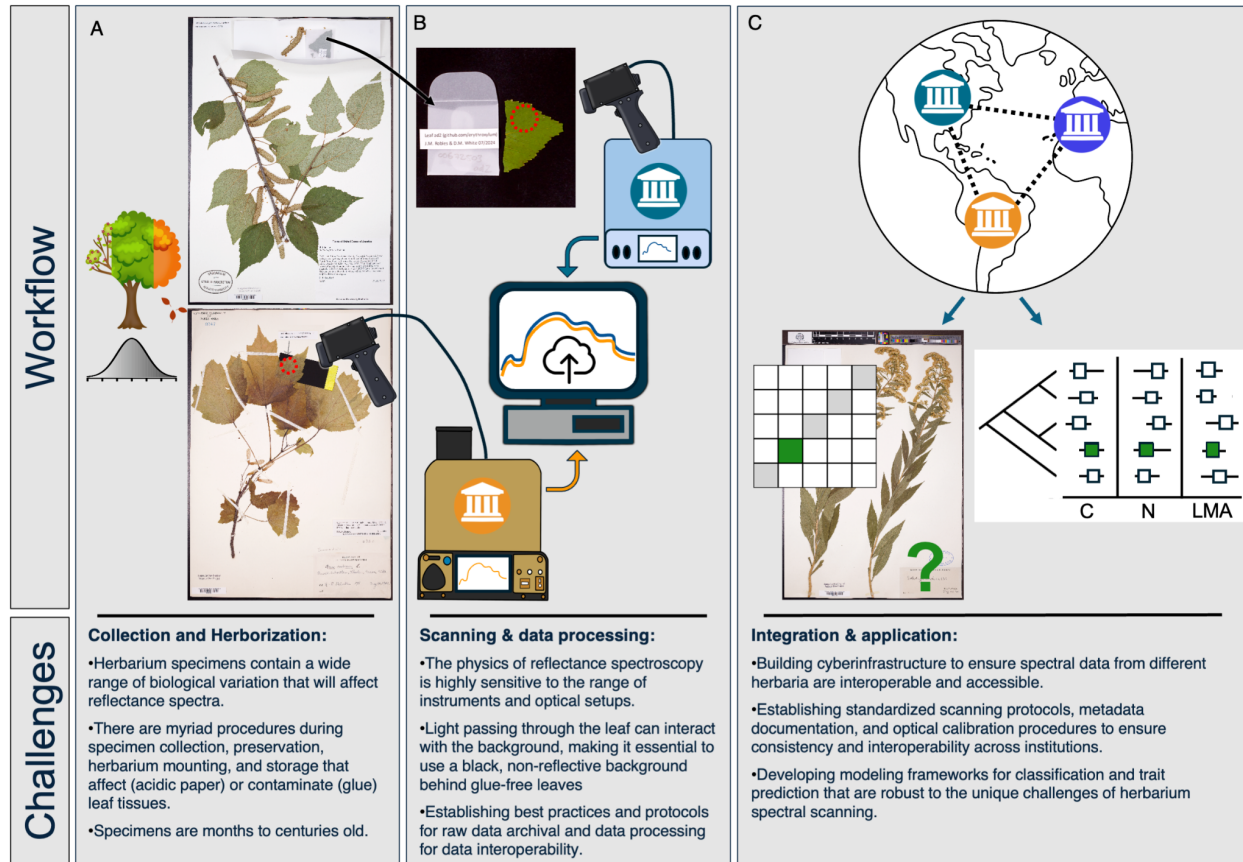
90 Several studies have now used pressed leaves (*i.e.* collected, dried, pressed, and stored in
91 newsprint) for trait prediction and taxonomic classification with remarkable success (Durgante *et al.*,
92 2013; Costa *et al.*, 2018; Kothari *et al.*, 2023), yet this paper, along with the investigation by Neto-
93 Bradley *et al.* presented in this special issue, are the first to investigate actual herbarium specimens. As
94 such, our primary questions are: To what extent can herbarium spectra complement fresh or pressed leaf
95 spectra in estimating traits and classifications? How do specimen-specific qualities like age or
96 preservation techniques influence the utility of spectral data? What next steps are necessary to optimize
97 sampling strategies, scanning protocols, and digital infrastructure for global data integration?

98 This study addresses whether herbarium specimens can serve as a reliable resource for reflectance
99 spectroscopy and exploring the biological signal integrity of these samples. We do this by building off of
100 the trait prediction and taxonomic classification work by Kothari *et al.* (2023), where 618 leaf samples
101 representing 67 species of North American trees, shrubs, and herbs plus one Australian species were
102 assayed for 22 functional traits before being reflectance scanned. The dried and pressed vouchers of these
103 samples were scanned using a PSR+ spectroradiometer with leaf clip (Spectral Evolution Inc.) after six
104 months to three years of storage time. Reanalysis of this dataset at 5 nm resampled bands (for
105 comparability) confirmed that pressed-leaf spectra excelled at predicting LMA ($R^2 = 0.94$; %RMSE =
106 6.29%), carbon ($R^2 = 0.79$; %RMSE = 10.10%), and cellulose ($R^2 = 0.77$; %RMSE = 7.80%), along with
107 moderate success for water-related traits, some nutrients, and pigments. Taxonomic classification models
108 achieved excellent accuracy (91%) for 10 species ($N > 20$), demonstrating the viability of pressed-leaf
109 spectra for functional trait estimation and species identification without destructive sampling.

110 Here, we have targeted 25 of the most well-sampled species in the pressed-leaf dataset for
111 scanning at the Harvard University Herbaria. This provides a comparative framework to test the utility of
112 herbarium specimens for predicting leaf mass per area (LMA) and for taxonomic classification. Leaf mass

113 per area was the best-predicted trait for the pressed-leaf models and does not require destructive sampling
114 to measure on herbarium specimens, when detached leaves are available. Additionally, this approach
115 permitted evaluation of the transferability of the pressed-leaf trait estimation models, which predict the
116 values of functional traits as they existed in vivo, to our herbarium spectra. Our goal here was to
117 understand just how different the models generated from pressed or herbarium leaves would be as a proxy
118 for understanding the changes herbarium leaf tissues undergo during preservation and storage. Finally, we
119 investigated whether specific herbarium specimen qualities, such as age, greenness, and the presence of
120 glue, were correlated with the success of taxonomic classification.

121 Our work seeks to form and refine a vision of herbarium-based spectral scanning as a promising
122 method for inferring plant traits within and across undersampled clades, and to begin to build spectral
123 databases that will be used in a variety of biodiversity science applications. This will also clarify the
124 limitations and opportunities inherent in using herbarium spectra, emphasizing the need to refine
125 methodologies and outline the scaled use of herbarium spectra in biodiversity science. By leveraging this
126 powerful technology with the amazing plant diversity collections in herbaria, we can establish a next
127 generation of digital resources that will be efficiently applied to pressing challenges in ecological and
128 evolutionary research.



129
 130 Fig. 2: The herbarium spectral scanning workflow from specimen collection to global integration,
 131 and challenges. **A)** The biological variation, specimen collection, and herborization factors affecting leaf
 132 spectra. Herbaria capture natural variation of plant tissues due to ontogeny, phenology, and plastic
 133 responses to abiotic and biotic factors. Along with this natural variation, the range of protocols employed
 134 to collect, preserve, and store specimens in herbaria influence tremendous variation in tissue preservation.
 135 Herbarium users observe a range of green (top) to brown (bottom) to black leaves and other
 136 characteristics reflecting tissue degradation or damage. Specimens have been mounted to different types
 137 of herbarium paper via glue (top), tape (bottom), or sewing. Loose leaf fragments held in envelopes (top)
 138 might be the only source of glue-free tissue for spectral applications. These specimens are to be preserved
 139 in perpetuity, but tissues will continue to change as they are used for research activities and experience
 140 environmental fluctuations as they age within herbaria across the globe. Top specimen from A:
 141 Herbarium of the Arnold Arboretum of Harvard University; bottom specimen from ECON: The
 142 Economic Herbarium of Oakes Ames of Harvard University. **B)** Scans taken with different instruments
 143 will inevitably be different. Spectroradiometers vary in spectral range, resolution, and signal-to-noise
 144 ratio, and even measurements taken with the same instrument model are affected by the optical
 145 components — e.g., light sources, lenses, and probe geometry — and instrument settings (e.g. integration
 146 time). The background against which leaves are scanned significantly affects the spectral signal and we
 147 currently do not have robust methods to unmix leaf spectral signals from the herbarium paper and glue, so
 148 herbarium leaves should be scanned against a standardized black background. This is done using detached
 149 leaves stored in labeled packets (top) or by carefully sliding a black background under glue-free leaves
 150 taped or sewn onto the herbarium sheet (bottom). Spectral data processing — e.g. scaling, band
 151 resampling, and applying mathematical transformations (e.g., wavelet transformations) — can be useful

152 but also introduce unintended biases and variation, so the raw spectra should always be made publicly
153 available. C) The vision of integrating herbarium spectral data into a global Metaherbarium, enabling
154 interoperable networks that connect institutions and support transformative scientific applications, such as
155 functional trait estimation and taxonomic discrimination. Achieving this vision relies on standardized
156 scanning protocols, optical procedures, and instrumentation, along with robust cyberinfrastructure to
157 aggregate and harmonize spectral data across herbaria, ensuring compatibility for downstream analyses.
158 These efforts lay the groundwork for advancing modeling frameworks capable of addressing biological
159 variation across the plant tree of life, while accounting for spectral changes introduced during
160 herborization and specimen aging. Such advancements will bridge herbarium collections with ecological
161 and evolutionary research, ushering in a new era of integrative biodiversity science. Specimen from
162 NEBC: The New England Botanical Club Herbarium.

163

164 Methods

165 Sampling design

166 Harvard University Herbaria (HUH) collections metadata for 68 species were obtained from the Global
167 Biodiversity Information Facility (GBIF.org) database using the R package `rgbif` v.3.8.0 (Chamberlain *et*
168 *al.*, 2024). To minimize geographic variation in traits that could affect trait comparisons, we targeted
169 collections from New England (Connecticut, Maine, Massachusetts, New Hampshire, Rhode Island, and
170 Vermont). This contrasts with the geographic scope of Ontario and Quebec in Kothari *et al.* (2023). The
171 one exception in both datasets is the species *Agonis flexuosa* from Australia. We first inspected all
172 specimens per species and selected specimens holding loose leaves in packets. If we were not able to get a
173 minimum of 15 specimens with loose leaves, we obtained permission from Lisa Standley, curator of the
174 New England Botanical Club Herbarium and Michaela Schnull, Director of Collections for the remaining
175 herbaria, to detach one leaf for scanning against the black background and measuring LMA. If multiple
176 leaves were available, we selected leaves without any sign of glue, but otherwise tried to randomly
177 sample with respect to the visual quality and degree of degradation across specimens.

178 Scanning Protocol

179 Specimens were scanned using a Spectra Vista Corporation HR 1024i spectroradiometer (350–2,500 nm
180 spectral range) with a fiber optic cable connected to the LC-RP Pro Leaf Clip/Reflectance Probe with a
181 narrow-angle lens, which reduced the scanning aperture to a 6 mm x 4 mm ellipse. The instrument was
182 turned on for a minimum of 10 minutes prior to scanning to allow the light source to warm and the
183 sensors to cool. At the beginning of each session, black card stock sprayed with three coats of Krylon®
184 Camouflage Black Matte spray paint was target-scanned three times to record a black background
185 spectrum for downstream quality control (not applied here) and then we took a reflectance scan on a
186 white Spectralon® reference panel. For each sample, we placed the leaf on top of the spray-painted black
187 cardstock and took three two-second scans of the adaxial surface. As an extra precaution against scanning
188 light reflected from the herbarium bench, the cardstock and leaves were scanned on top of a 5 mm felt pad
189 coated with the same matte black spray paint. We targeted regions of the leaf that avoided the midvein,
190 prominent secondary veins, or regions with disease, fungus, or other damage. Up to two leaves per
191 specimen were scanned. Finally, a second target scan of the white Spectralon® panel was taken for
192 downstream quality control (not applied here).

193 Trait Measurements

194 Leaf weight, area, and thickness were recorded for each scanned leaf to validate leaf mass per area
195 (LMA) predictions from spectra. After scanning, petioles were removed at the point of contact with the
196 leaf lamina or slightly above the midpoint of acuminate leaf bases. Leaf blade weight was measured in
197 milligrams using a Sartorius Practum64-1S Analytical Balance. Petioles were stored in glassine envelopes
198 with labeled scan numbers. Leaf area was measured using the LeafByte® app on an iPhone 15 with five
199 or 10 cm² calibration dots.

200 Spectra Preprocessing

201 To ensure compatibility with downstream analyses and comparability of results across datasets,
202 we reprocessed and reanalyzed the raw pressed leaf spectra of Kothari *et al.* (2023) in addition to the
203 herbarium leaf spectra. Raw spectra files were processed using the SpectroLab v. 0.0.18 R package
204 (Meireles *et al.*, 2017). We resampled reflectance spectra to 5 nm intervals using the Full-Width Half-
205 Maximum (FWHM) method in the CWT R package (Guzmán Q., 2024) to make the spectral resolution
206 consistent, as the two datasets were generated on different sensors with different resolutions.

207 With the goal of optimizing the transferability of models across spectral datasets, the resampled
208 reflectance spectra in each dataset were then transformed using two methods: vector normalization and
209 continuous wavelet transformation (CWT). Vector normalization of the spectra was implemented as a
210 method to reduce the impact of differences in illumination geometry between spectrometers, which can
211 impact the magnitude of reflectance. This method was applied using the ‘normalize’ function of
212 SpectroLab. Continuous wavelet transformation (CWT) was implemented as a method to isolate scales
213 that capture spectral features, potentially enhancing the prediction of leaf traits and the transferability of
214 models (Guzmán Q. & Sanchez-Azofeifa, 2021). This method is based on the premise that the leaf
215 reflectance spectra can be expressed as a combination of wave-like functions (wavelets) of varying scales
216 (widths), enhancing fine spectral features at lower scales and broader spectral patterns at large scales
217 (Rivard *et al.*, 2008). We applied this transformation on the resampled leaf reflectance from both datasets
218 using a second-order Gaussian derivative wavelet function and applying a variance of 1. The choice of
219 wavelet scales can impact the predictive performance of predicting models (Guzmán Q. & Sanchez-
220 Azofeifa, 2021). Based on exploratory analysis, scales 2^2 , 2^3 , and 2^4 were computed and summed to form
221 the summed-wavelet spectra used for predicting leaf traits. The CWT transformation was implemented
222 using the ‘cwt’ function from the *CWT* package in R (Guzmán Q., 2024).

223 The resulting reflectance spectra (e.g., reflectance, vector normalized, and summed-wavelet) were
224 trimmed to a range of 450–2,400 to remove noisy regions at the spectrum's edges. The 400–450 nm range

225 was removed because reflectance values in this region differed substantially between the herbarium and
226 pressed leaf datasets. We also subdivided the data into different spectral regions: 450–1,300nm as the
227 visible and near-infrared (VNIR+) region (“+” because 1,100–1,300 nm is in the short-wave infrared) that
228 could be noisier due to pigment degradation (Fourty *et al.*, 1996), and the 1,350–2,400 nm short-wave
229 infrared region.

230 Prediction of LMA

231 Using the processed spectra and the measured leaf mass per area (LMA; kg m⁻²) from each of the
232 pressed and herbarium datasets across the VNIR+ (450-1,300 nm), SWIR, and full-range spectral regions,
233 we built predictive models using partial least squares (PLS) regression implemented with the *pls* and
234 *caret* R packages (Liland *et al.*, 2024b; Kuhn *et al.*, 2024). Metadata and spectral data were split into
235 training (75%) and validation (25%) datasets using a stratified sampling approach based on growth form,
236 mirroring Kothari *et al.* (2023). We generated 1,000 model segments by randomly selecting individual
237 scans for each specimen using a custom data segmentation function. This procedure ensured that scans
238 from each specimen were never split among both the training and validation datasets while capturing the
239 variability within specimens and avoiding bias introduced by the averaging of spectra.

240 Model optimization was performed using a custom tuning function that used cross validation with
241 the ‘oscorepls’ method. The predictive residual sum of squares (PRESS) metric was used to evaluate the
242 models during cross-validation and the optimal number of components for the PLS regression models was
243 selected as the smallest value whose PRESS value was within one standard deviation of the minimum
244 PRESS value.

245 Final models were constructed using the optimal number of components and validated on the
246 independent test datasets. We evaluated our predictions using the full ensemble of model segments,
247 averaged to each individual, and predictions of LMA were compared to observed values to calculate
248 residuals and evaluate performance. The model performance was evaluated by estimating the coefficient
249 of determination (R^2), the bias, the root mean squared error (RMSE), and the percentage RMSE (%RMSE
250 = RMSE/ range of 0.99 and 0.01 quantiles). Finally, we calculated variable importance in projection
251 (VIP) values to estimate the most informative spectral regions, and extracted model coefficients for
252 making predictions across external datasets – permitting our tests of model transfer between the pressed
253 models to herbarium spectra and vice versa. Lastly, we used the trait data presented in Kothari *et al.*
254 (2023) to generate PLSR models in the same manner as for LMA in order to use the model coefficients
255 and intercept to predict trait values from the herbarium leaf spectra for carbon, calcium, carotenoids,
256 cellulose, chlorophyll A, LMA, nitrogen, and solubles. To assess the accuracy of model transfers for these

257 other traits for which we have no observed herbarium trait values, we compared the distributions of
258 predicted herbarium trait values against the observed values from Kothari *et al.* (2023).

259 To further evaluate transferability, we applied model coefficients derived from one dataset to
260 spectra from the other. Using the transformed reflectance data, predictions were generated, and their
261 accuracy was assessed by calculating residuals and comparing predicted vs. observed values. This step
262 validated the applicability of standardized coefficients across datasets and quantified the degree of
263 compatibility between herbarium and pressed leaf spectra.

264 Taxonomic Classification

265 To test the viability of models classifying herbarium leaf scans into taxa, we applied partial least squares
266 discriminant analysis (PLS-DA) and linear discriminant analysis (LDA) to the reflectance spectra of the
267 full-range herbarium spectral dataset, without any vector normalization or continuous wavelet
268 transformations. We tested both the PLS-DA and LDA algorithms because, although they are both
269 implemented by different research groups, we are not aware of any studies that have directly compared
270 their results. PLS-DA uses partial least squares regression to reduce dimensionality and optimize feature
271 selection, making it suitable for high-dimensional datasets like spectra, especially in scenarios with few
272 samples compared to many predictors (high-dimensional low-sample-size problems). This method
273 requires researchers to specify the number of components used by the model, demanding a careful
274 balance between improving accuracy and avoiding overfitting to the training dataset. LDA, in contrast,
275 assumes normally distributed data and separates classes by maximizing variance between groups, offering
276 robust classification in well-distributed datasets without the need to specify a number of components.
277 LDA is also computationally much lighter than PLS-DA.

278 Classification models were built using the *caret*, *pls*, and *plsVarSel* packages in R (Liland *et al.*,
279 2024a,b; Kuhn *et al.*, 2024). First, spectral data were preprocessed by splitting the dataset into ten
280 individuals per species selected for training and the rest for validation, ensuring balanced representation
281 across species. The same segmentation process as above was employed to generate 1,000 data segments
282 for iterative training and testing across spectral scans.

283 For PLS-DA, model tuning was performed with the PLS method and optimized by the
284 classification accuracy metric. We generated final models across our 1,000 data segments by selecting the
285 number of components returning the highest classification accuracy. LDA models were generated with
286 the ‘LDA’ method optimized by the accuracy metric.

287 Model performance was assessed using the independent test datasets by generating confusion
288 matrices to calculate accuracy, sensitivity, and specificity metrics. We also generated variable importance
289 in projection (VIP) scores from the models to identify the most influential spectral regions for

290 distinguishing taxa, and extracted and saved coefficients from the PLS-DA models for generating class
291 predictions and prediction probabilities from all specimens for an analysis of factors that influence
292 classification success.

293 Analysis of specimen predictors on classification

294 To evaluate the biotic and herborization factors influencing the success of PLS-DA classification, we
295 utilized the full ensemble of 1,000 optimized PLS-DA models trained on the full-spectrum herbarium
296 dataset of 25 species. Using the model coefficients, x-values, and y-values (intercepts), we computed
297 classification probabilities for all 1,690 herbarium leaf scans across the ensemble of models. Probabilities
298 were averaged across all models, and the predicted class was determined as the one with the highest
299 average probability.

300 These predictions were integrated with specimen metadata to conduct a series of comparisons and
301 independent regressions of classification probabilities against categorical variables (specimen quality,
302 glue presence, observed damage, and leaf developmental stage) and numerical variables (age, Julian day
303 of collection, nearest taxon distance, LMA, and greenness index). Descriptions of predictor variables are
304 provided in Table 1.

305 To estimate nearest taxon distance, a phylogram was made using Time Tree 5 (timetree.org;
306 (Kumar *et al.*, 2022) with modifications following results from V.PhyloMaker2 (Jin & Qian, 2022) to add
307 *Phragmites australis* as sister to *Phalaris arundinacea* at 39.8 My and add *Betula populifolia* as sister to
308 *Betula papyrifera* at 39.7 My. Greenness index, which measures the relative difference in reflectance
309 between green light (550 nm) and red light (690 nm; see equation in Table 1), was selected over other
310 commonly used vegetation indices, such as normalized difference vegetation index, green normalized
311 difference vegetation index, and chlorophyll/carotenoid index, due to its significant correlation with the
312 independent estimate of specimen quality (Fig. S1). Relationships and regressions were visualized using
313 the ggplot2 package in R (Wickham *et al.*, 2024), and significant differences in classification probabilities
314 between correct and incorrect classes were assessed using t-tests as implemented by the ‘ggsignif’ function
315 in ggplot2.

316 Logistic regression and random forest analyses were performed to further evaluate significant
317 relationships between specimen metadata and classification accuracy. The logistic regression model,
318 implemented with the ‘glm’ function in the stats R package (R Core Team, 2023), employed a binomial
319 error structure and included all predictors. For the random forest analysis, the randomForest R package
320 (Breiman *et al.*, 2024) was used to quantify predictor importance based on mean decrease in accuracy and
321 Gini impurity metrics.

322

323 Table 1: Metadata predictors of herbarium specimens and descriptions of classes.

Metadata predictor	Class	Description
Leaf Developmental Stage	Young	Thin leaves with under-developed venation, prone to bruising, may appear darker, scans usually have lower reflectance. Collection date is important.
	Mature	Typically thick leaves, with potential color differences between adaxial and abaxial surfaces.
	Senescent (Not observed)	Discolored leaves, often associated with aging. Collection date helps confirm senescence.
Leaf Damage	None	No visible pre- or post-mortem damage to leaves.
	Minor	Damage present on some leaves but not affecting scanned regions.
	Medium	Minor damage visible on scanned leaves, but likely not in the scanned regions.
	Major	Significant damage is visible in the scanned regions.
Specimen Quality	Good	Resembles a freshly pressed specimen.
	Medium	Shows some discoloration but is otherwise intact.
	Poor	Highly degraded specimen, with discoloration, mold, or rugosity from wilting.
Glue	Present	Specimen preparation involved glue application.
	Absent	No glue was used during specimen preparation.
Green Index	(Numerical)	$\text{Green Index} = \frac{\text{Reflectance}_{550\text{nm}} - \text{Reflectance}_{690\text{nm}}}{\text{Reflectance}_{550\text{nm}} + \text{Reflectance}_{690\text{nm}}}$
Age	(Numerical)	Years since specimen was collected (mean = 94)
Day of Year	(Numerical)	Julian day of collection
Leaf Mass per Area	(Numerical)	Kg m^{-2}
Nearest Taxon Distance	(Numerical)	Estimated age (in millions of years) of most recent common ancestor shared between predicted taxon and nearest sampled species.

324

325

326 Results

327 Trait prediction & model transferability

328 Spectral profiles of 25 species scanned from the Harvard University Herbaria have similar
329 profiles but lower magnitudes compared to pressed leaves (Fig. 3A). Within herbarium spectra, we also
330 observe notable variation in the coefficient of variation of reflectance within the visible (450-700 nm) and
331 SWIR regions (specifically ~1,900-2,400); Fig. S2). Models trained on herbarium spectra using all
332 combinations of spectral transformations (untransformed, vector-normalized, and CWT) and wavelength
333 ranges (full, VNIR+, and SWIR) had excellent performance (validation tests in Table 2; full statistics in
334 Table S1).

335 Overall, the best validation models according to R^2 and %RMSE were the full-range, vector-
336 normalized models, but the models using untransformed reflectance values were only slightly less
337 accurate. For the non-transformed reflectance values, pressed LMA models performed only slightly better
338 than the herbarium LMA models (pressed $R^2 = 0.942$, %RMSE = 6.29%; herbarium $R^2 = 0.891$, %RMSE
339 = 6.62%, Fig. 4A and B). After full-range models, SWIR models performed better than VNIR+ (Table
340 S1).

341 As expected, the performance of models was reduced when they were transferred and validated
342 with the other (herbarium or pressed) LMA dataset, but the CWT and non-transformed reflectance models
343 could still accurately predict observed LMA (Table 2; Table S1; Fig. 4B and C). The best transfer model
344 was for the full-range CWT dataset (herbarium to pressed $R^2 = 0.88$, %RMSE = 8.76%; pressed to
345 herbarium $R^2 = 0.76$, %RMSE = 10.53%). The shifted slope of an ordinary least squares regression of
346 predicted values highlights a systematic difference in models between datasets (0.91 in Fig. 4C and 1.25
347 in Fig. 4D; transfer tests in Table 2). Models based on the VNIR+ spectra also performed well for
348 reflectance and CWT datasets, but SWIR-based models showed reduced performance (Table S1).
349 Contrasting with their improved performance in internal validation tests, the models based on vector-
350 normalized spectra performed worse than the other two spectral datasets, yet showed best performance for
351 models in the SWIR range (Table 2; Table S1).

352

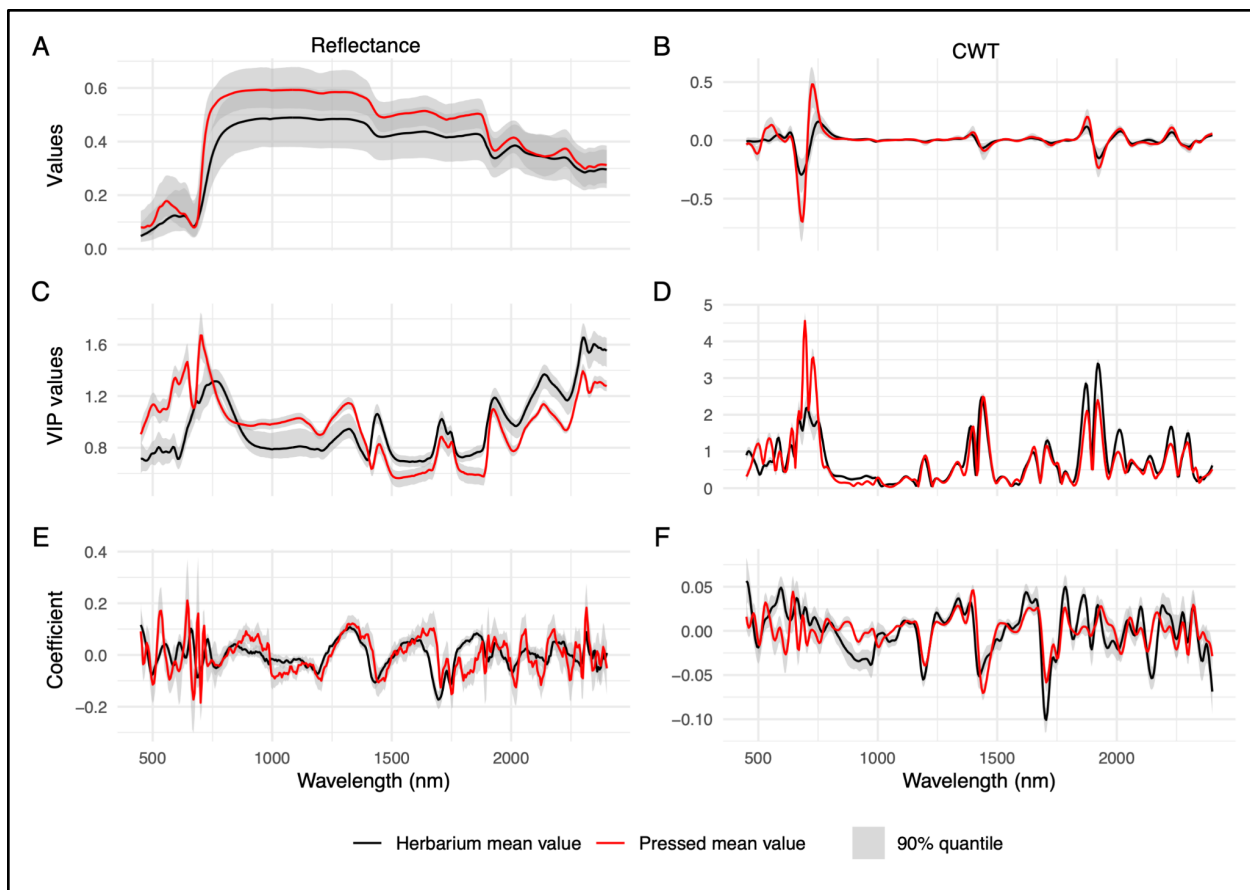
353

Table 2: Performance metrics for LMA models averaged across 1,000 model segments.

test	model	spectra	transform	N	Ncomponents	R ²	%RMSE	RMSE (Kg m ⁻²)	BIAS	slope	intercept
validation	herbarium	herbarium	CWT	220	10	0.81 ± 0.01	7.92 ± 0	0.011 ± 0	0 ± 0	1.00 ± 0.02	0 ± 0
validation	herbarium	herbarium	reflectance	220	14	0.89 ± 0.01	6.62 ± 0	0.01 ± 0	0 ± 0	0.99 ± 0.02	0 ± 0
validation	herbarium	herbarium	normalized	220	14	0.92 ± 0.01	5.79 ± 0	0.009 ± 0	0 ± 0	1.01 ± 0.01	0 ± 0
validation	Pressed	Pressed	CWT	212	8	0.94 ± 0	6.34 ± 0	0.011 ± 0	0 ± 0	1.03 ± 0.02	0 ± 0
validation	Pressed	Pressed	reflectance	212	16	0.94 ± 0	6.29 ± 0	0.011 ± 0	0 ± 0	1.02 ± 0.02	0 ± 0
validation	Pressed	Pressed	normalized	212	13	0.95 ± 0	6.01 ± 0	0.011 ± 0	0 ± 0	1.00 ± 0.02	0 ± 0
transfer	herbarium	pressed	CWT	609	14	0.88 ± 0.03	8.76 ± 0.02	0.015 ± 0	0 ± 0.01	0.91 ± 0.06	0.00 ± 0.01
transfer	herbarium	pressed	reflectance	609	14	0.91 ± 0.01	10.99 ± 0.02	0.019 ± 0	-0.01 ± 0.01	0.82 ± 0.02	0.00 ± 0.01
transfer	herbarium	pressed	normalized	609	14	0.91 ± 0.01	78.48 ± 0.5	0.136 ± 0.09	0.12 ± 0.11	1.47 ± 0.05	0.13 ± 0.16
transfer	pressed	herbarium	CWT	479	8	0.76 ± 0.05	10.53 ± 0.01	0.016 ± 0	0 ± 0	1.25 ± 0.06	-0.02 ± 0.01
transfer	pressed	herbarium	reflectance	479	16	0.66 ± 0.07	13.13 ± 0.02	0.02 ± 0	0.01 ± 0.01	1.13 ± 0.1	0.01 ± 0
transfer	pressed	herbarium	normalized	479	13	0.51 ± 0.09	781.00 ± 2.43	1.178 ± 0.37	-1.18 ± 0.37	0.41 ± 0.09	-0.41 ± 0.06

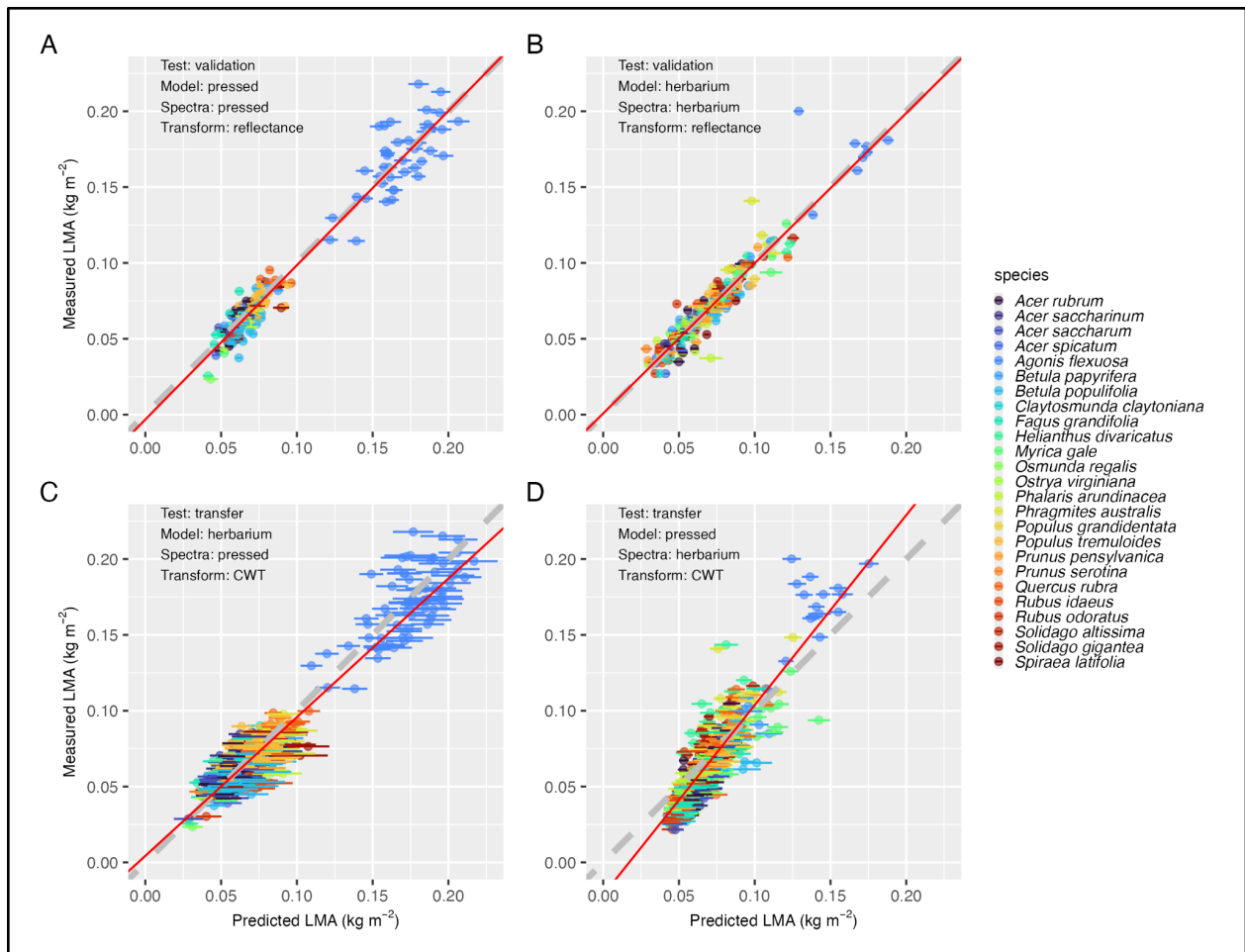
354

355



356
 357 **Fig. 3:** Plots of reflectance and CWT values for herbarium and pressed datasets, plus associated variable
 358 importance in projection (VIP) metrics and model coefficients for LMA models. Black lines represent
 359 mean herbarium data and red lines represent mean pressed data, with 90% quantiles plotted in gray bands.
 360 Panels show the data for (A) the reflectance data across all samples, (B) the CWT transformed reflectance
 361 data across all samples, (C) VIP values for reflectance data across 1,000 model iterations, (D) VIP values
 362 for CWT data across 1,000 model iterations, (E) Reflectance model coefficients across 1,000 iterations,
 363 (F) CWT model coefficients across 1,000 iterations.

364



365
 366
 367
 368
 369
 370
 371
 372
 373
 374

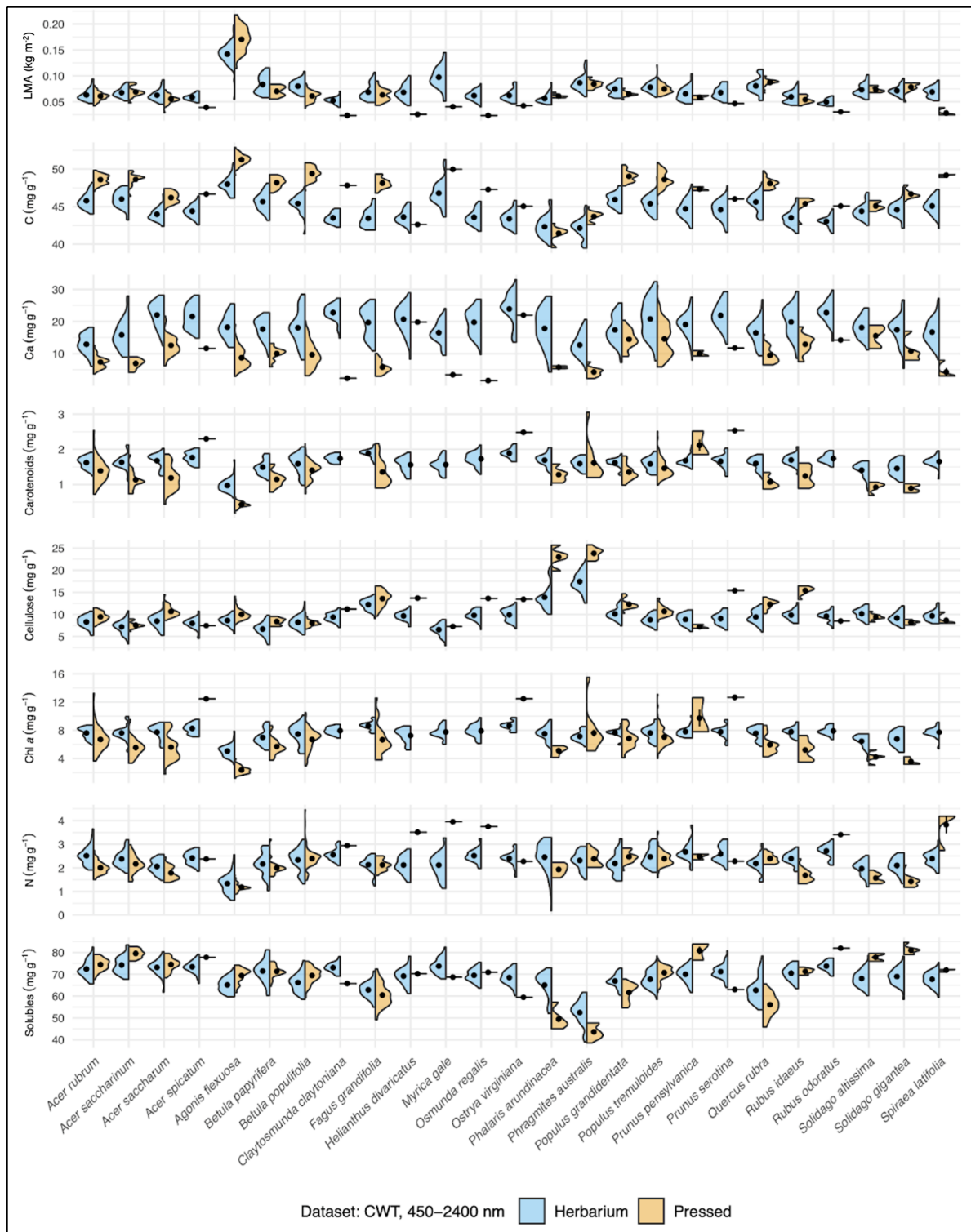
Fig. 4: Validation and model transfer results for leaf mass per area (LMA) per individual across 25 species. Error bars represent the standard deviation in predictions across 1,000 model iterations. Linear regressions of observed versus predicted values averaged across iterations are shown in red lines for comparison with the gray 1:1 dashed lines. Individual plots show the results for full-range spectra (450-2,500 nm) of (A) pressed models from untransformed reflectance values, (B) herbarium models from untransformed reflectance values, (C) transfer of CWT herbarium models to CWT pressed spectra, and (D) transfer of CWT pressed models to CWT herbarium spectra.

375 The compatibility of the models is further illustrated by the similarity of variable importance in
376 projection (VIP) values for reflectance spectra (Fig. 3C). The VIP plots reveal considerable differences
377 between herbarium and pressed models in the visible and (less-so) NIR regions, but the relative values in
378 the SWIR region are similar. This same pattern applies to the model coefficients (Fig. 3C). The CWT
379 models follow a similar pattern across the visible, NIR, and SWIR regions, yet with fewer differences
380 among peak patterns and overall closer magnitudes (Fig. 3D and F). The CWT models have the most
381 clearly defined peaks and highlight informative spectral regions throughout the spectral range (Fig. 3D
382 peaks = VIS: 500 nm, 545 nm, 590 nm, 640 nm, 670 nm, 695 nm; NIR: 730 nm; SWIR: 1,200 nm, 1,400
383 nm, 1,440 nm, 1,655 nm, 1,705 nm, 1,875 nm, 1,920 nm, 2,225 nm, 2,295 nm).

384 To extend this inference of the utility of transferring trait models, we applied seven additional
385 pressed-leaf trait models to predict traits from the herbarium spectra for 25 species (Fig. 5; validation
386 results in Table S2). The predicted trait distributions from herbarium spectra closely align with observed
387 distributions from the pressed dataset, highlighting the potential of these models for cross-dataset
388 applications. Predicted values for key traits, including leaf mass per area (LMA), carbon fractions, and
389 carotenoids, generally showed contiguous distributions with substantial overlap between datasets. This
390 overlap shows the robustness of the spectral models in maintaining rank-order consistency across species.
391 Discrepancies arose, particularly where pressed datasets included only a single individual per species and
392 model generalizability was limited, but the lack of unrealistic trait values and the general correspondence
393 of distributions across these additional traits is a surprisingly positive result.

394 These results taken together provide robust support for the utility of herbarium spectra for trait
395 estimation both for models built from herbarium-derived trait datasets as well as for the transfer of
396 pressed leaf models built from trait values measured in living plants.

397



398

399 **Fig. 5:** Comparison of observed trait distributions from pressed leaves with predicted values obtained by
 400 applying continuous wavelet transformation (CWT) pressed models to herbarium spectra, as shown in
 401 Fig. 2C. Panels display the distributions for eight traits across 25 species. Mean values are indicated with
 402 black dots.

403 Taxonomic Classification

404 To evaluate the utility of reflectance spectra for taxonomic classification, we applied linear
405 discriminant analysis (LDA) and partial least squares discriminant analysis (PLS-DA) models across
406 datasets at two taxonomic levels: species and genus. To ensure direct comparability of results, we also
407 analyzed the pressed leaf dataset for the ten species for which 20 or more individuals were sampled.
408 Performance metrics, including accuracy, precision, and balanced accuracy, were compared to assess the
409 classification capabilities of each approach.

410 Pressed datasets outperformed herbarium datasets in classification accuracy, precision, and
411 balanced accuracy, yet herbarium spectra still provided reliable classification models (Table 3). In the 10-
412 species dataset, pressed specimens achieved accuracies of $91.7 \pm 2\%$ (LDA) and $81.1 \pm 2\%$ (PLS-DA),
413 while herbarium specimens achieved $71.9 \pm 2\%$ (LDA) and $58.0 \pm 2\%$ (PLS-DA).

414 For the 25-species dataset, herbarium spectra achieved $74.3 \pm 1\%$ accuracy with PLS-DA,
415 outperforming LDA's $64.4 \pm 2\%$. The confusion matrix (Fig. 5) shows that most classification errors
416 occurred between congeneric species, highlighting challenges in distinguishing closely related taxa. Some
417 species, such as *Osmunda regalis* and *Quercus rubra*, were frequently misclassified as *Betula* species.
418 Notably, *Solidago gigantea* had a correct classification rate of only 39%, with 51% of its scans
419 misclassified as *Solidago altissima*. The variable importance in projection (VIP) plots are consistent
420 across species and emphasize key spectral regions in the visible, near-infrared, and shortwave infrared
421 (SWIR) ranges (Fig. S3).

422 At the genus level, pressed specimens achieved near-perfect accuracy in the six-genera dataset,
423 with $96.9 \pm 1\%$ (LDA) and $89.8 \pm 1\%$ (PLS-DA), while herbarium specimens achieved $89.3 \pm 2\%$ (LDA)
424 and $82.1 \pm 1\%$ (PLS-DA). In the more complex 17-genus dataset, herbarium spectra performed better
425 with PLS-DA ($84.9 \pm 1\%$) compared to LDA ($75.3 \pm 2\%$). Similarly, PLS-DA outperformed LDA in the
426 17-genus dataset, achieving $84.9 \pm 1\%$ for PLS-DA compared to $75.3 \pm 2\%$ for LDA.

427 The VIP plots comparing herbarium and pressed datasets reveal consistent peaks across the
428 visible, near-infrared, and shortwave infrared (SWIR) regions, reflecting the spectral regions most
429 important for PLS-DA classification (Fig. S4).

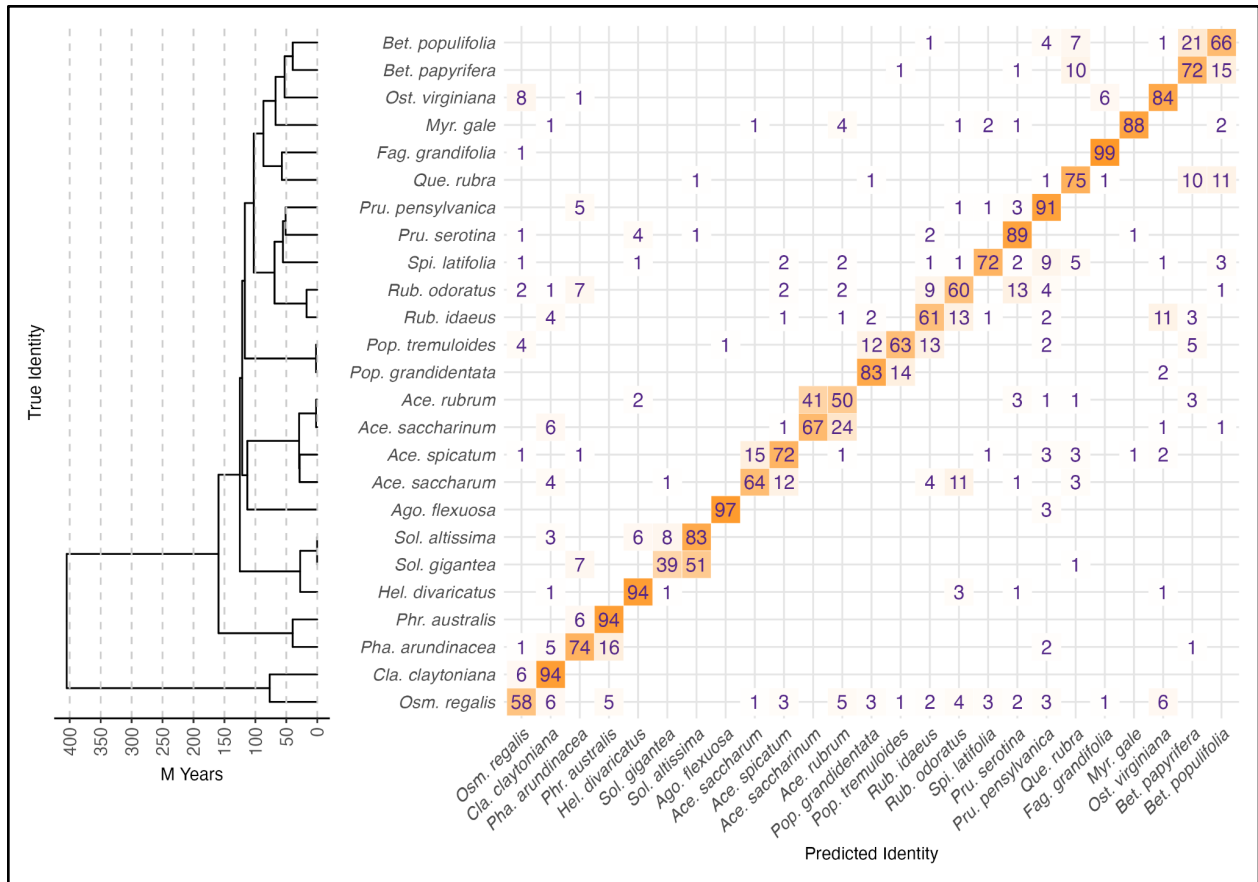
430

431 Table 3: Performance metrics of classification analyses

Dataset	Rank	Model	Samples	Ncomponents	Accuracy \pm SD (%)	Precision \pm SD (%)	Balanced Accuracy \pm SD (%)
Herbarium	species	LDA	10 spp	<i>N/A</i>	71.9 \pm 2	72.1 \pm 20	84.2 \pm 10
Herbarium	species	PLSDA	10 spp	15	58 \pm 2	58.5 \pm 23	76.5 \pm 13
Pressed	species	LDA	10 spp	<i>N/A</i>	91.7 \pm 2	86.6 \pm 20	96.3 \pm 3
Pressed	species	PLSDA	10 spp	15	81.1 \pm 2	73.2 \pm 22	91.7 \pm 6
Herbarium	genus	LDA	6 genera	<i>N/A</i>	89.3 \pm 2	87.8 \pm 14	92.8 \pm 7
Herbarium	genus	PLSDA	6 genera	13	82.1 \pm 1	79.5 \pm 21	86.8 \pm 12
Pressed	genus	LDA	6 genera	<i>N/A</i>	96.9 \pm 1	94.6 \pm 10	98.3 \pm 2
Pressed	genus	PLSDA	6 genera	13	89.8 \pm 1	85.2 \pm 13	93.9 \pm 5
Herbarium	species	LDA	25 spp	<i>N/A</i>	64.4 \pm 2	67.2 \pm 19	82 \pm 9
Herbarium	species	PLSDA	25 spp	24	74.3 \pm 1	75.3 \pm 15	87.3 \pm 8
Herbarium	genus	LDA	17 genera	<i>N/A</i>	75.3 \pm 2	76.5 \pm 18	86.4 \pm 8
Herbarium	genus	PLSDA	17 genera	27	84.9 \pm 1	87 \pm 8	90.9 \pm 9

432

433



434

435 **Fig. 6:** Phylogram and confusion matrix summarizing the validation of herbarium specimen classification
 436 using Partial Least Squares Discriminant Analysis (PLS-DA). The left panel shows a phylogram
 437 representing the evolutionary relationships among species scaled by millions of years. The right panel
 438 displays a confusion matrix where rows represent true species identities and columns represent predicted
 439 species identities. Tile colors indicate the percentage of observations of each pair of true and predicted
 440 identities, with darker shades representing higher percentages. Numbers within tiles show rounded
 441 percentages. Mean accuracy for the validation is 74.3%.

442

443 Assessing herborization factors on classification

444 To evaluate the influence of specimen factors on PLS-DA classification performance, we analyzed the
445 classification probabilities across all 1,690 herbarium scans using the full-spectrum 25-species dataset
446 (Fig. S5). Logistic regression and independent t-tests revealed significant relationships between
447 classification probabilities and several categorical and numerical predictor variables.

448 The probabilities of correct classifications varied significantly with specimen quality, glue
449 presence, leaf damage, and leaf phenological development (Fig. 7). Leaves with good ($p < 0.001$) or
450 medium quality ($p < 0.01$) had higher predicted probabilities for correct classifications compared to those
451 with poor quality, but there was not a significant difference between good and medium quality specimens.
452 Following expectations, specimens without mounting glue had significantly higher predicted probabilities
453 than those with glue ($p < 0.001$). Mature leaves exhibited higher predicted probabilities compared to
454 young leaves ($p < 0.001$). Probabilities of correct classifications for specimens with no damage were
455 significantly higher than those with minor damage ($p < 0.001$) and medium damage ($p < 0.05$), as well as
456 between minor and major - but in the opposite direction of expected ($p < 0.05$). The few specimens with
457 major damage had curiously high classification probabilities. The probabilities of incorrect classifications
458 – which represent the individual false-positive classifications that had higher probabilities than true-
459 positives – did not significantly differ across classes within these variables (Fig. 7).

460 Numerical predictors also had significant relationships with classification probabilities (Fig. 8).
461 Age negatively correlated with classification probabilities, suggesting reduced model performance for
462 older specimens (Fig. 8A). The age of the sampled specimens ranged from one to 179 years with a
463 median age of 91 years (Fig. S6). The green index was also negatively correlated with classification
464 probabilities, indicating that greener leaves were related to worse model performance (Fig. 8B). The
465 relationship between age and green index revealed that older specimens generally exhibited lower green
466 index values, consistent with expected tissue degradation over time (Fig. 8C).

467 Classification probabilities increased with greater phylogenetic distance to the nearest taxon (Fig.
468 8D), an expected relationship that corroborates the results of the confusion matrix. Conversely, the
469 probability of a false positive classification decays with phylogenetic distance to the predicted class (Fig.
470 S7). Leaf mass per area also shows a strong positive correlation with classification probability (Fig. S8)
471 with the caveat of covariation with species composition. *Agonis flexuosa* was classified with an overall
472 accuracy of 97% and LMA values for this species are outstanding within this dataset.

473 Logistic regression taking into account phylogeny (Table 4) further supported these factors as
474 important in classification success. As expected, the most influential metric in classification success is
475 nearest taxon distance, but the next most significant predictors were age, green index, absence of glue,
476 and specimen quality. Finally, there is a weak positive relationship with classification success (Table 4)

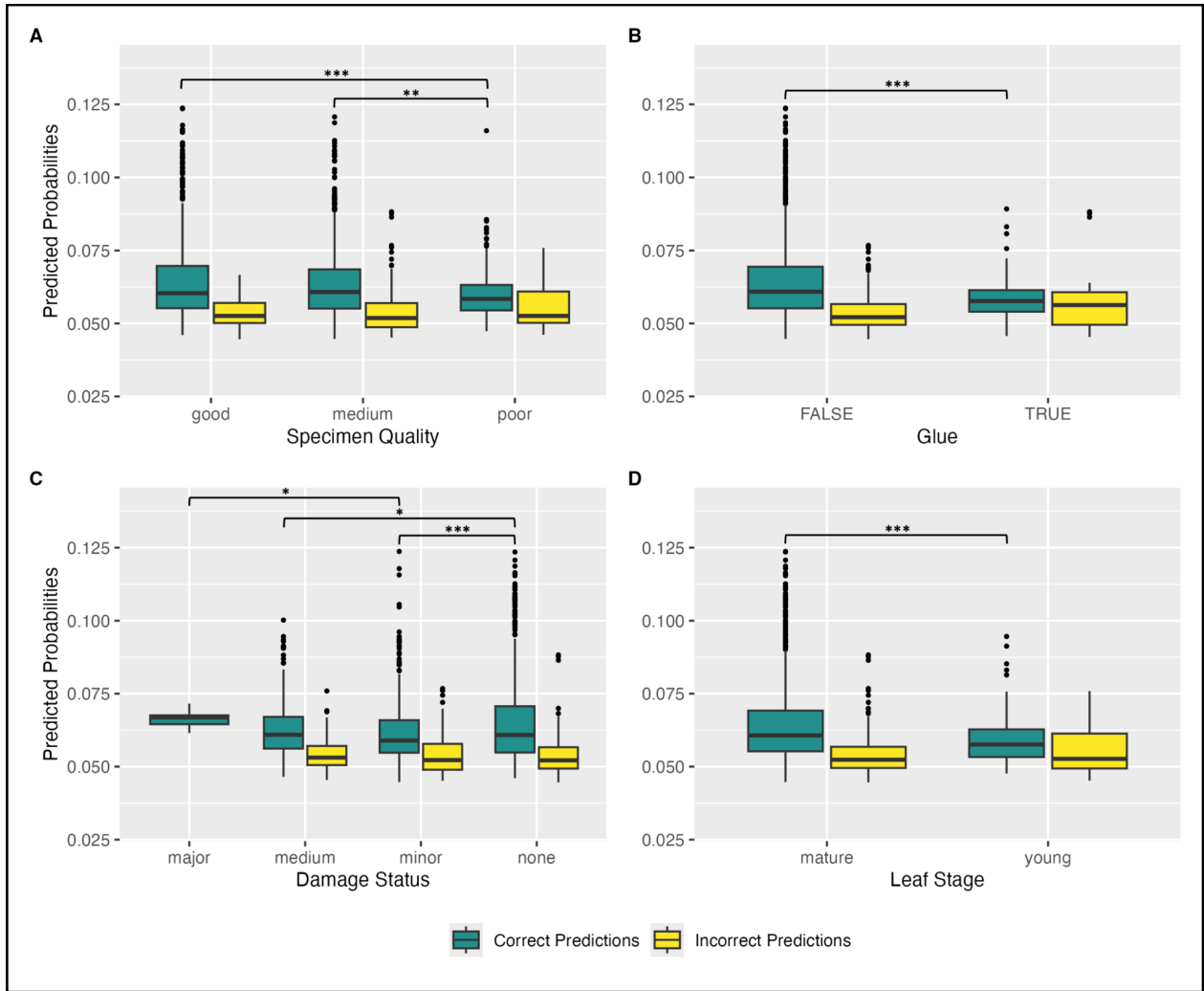
477 and classification probability (Fig. S9) with the calendar day of specimen collection. This provides weak
 478 support that species collected early in the growing season were more likely to be misclassified than those
 479 collected at later dates. Random forest models generally corroborated these results, but optimized LMA,
 480 Age, and the green index as more significant factors than nearest taxon distance (Table S3).

481 These results highlight the critical influence of specimen metadata on PLS-DA classification
 482 performance. Factors such as tissue integrity, as measured by the green index, and phylogenetic
 483 distinctiveness strongly impact classification success. In contrast, older specimens, poor-quality leaves,
 484 and the presence of glue reduce classification probabilities, underscoring the importance of these
 485 metadata for optimizing model performance.

486 Table 4: Logarithmic regression of all predictors.
 487

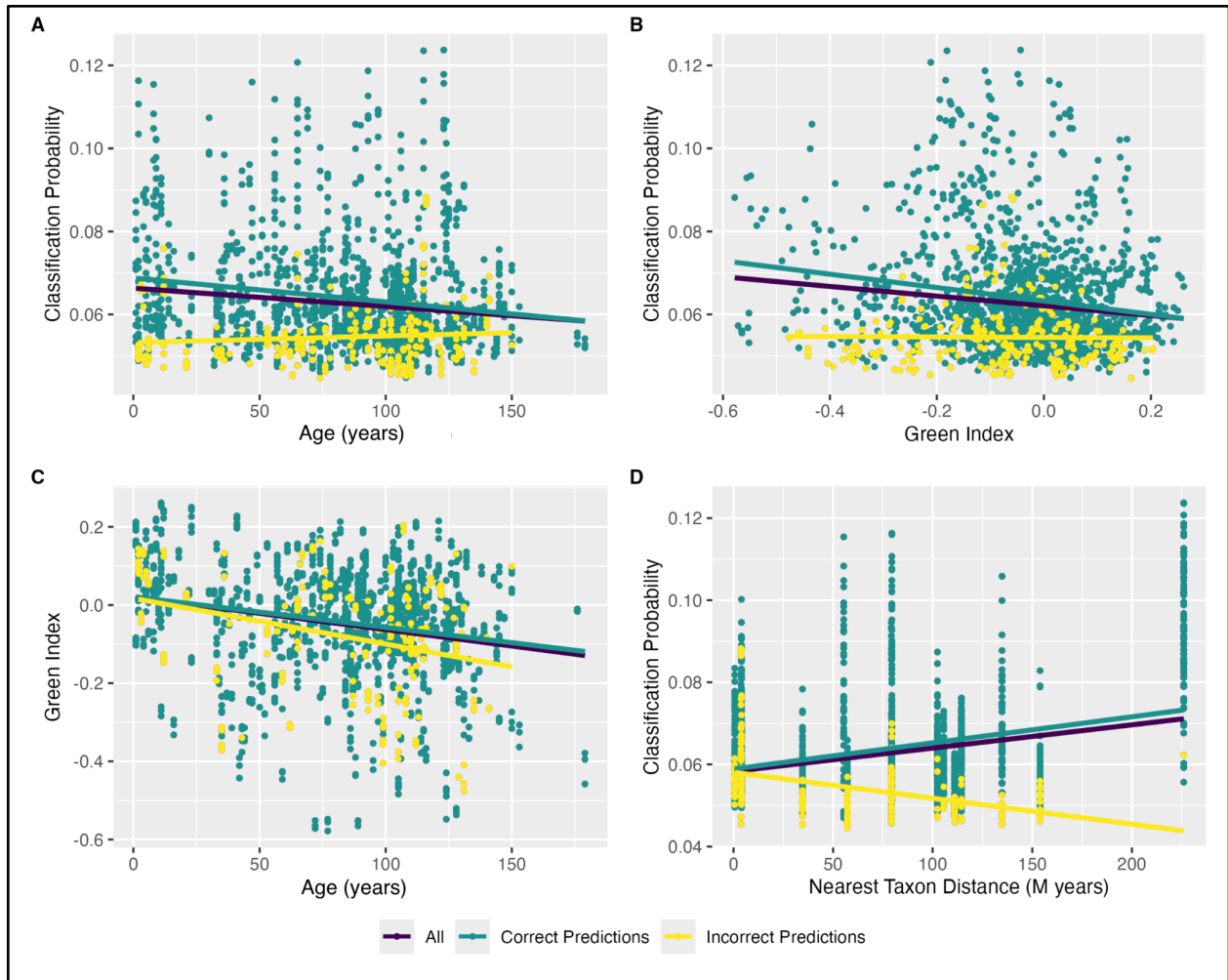
	Estimate	Std. Error	z value	Pr(> z)	Sig.
(Intercept)	1.18E+01	3.60E+02	3.29E-02	9.74E-01	
Nearest Taxon Distance	8.15E-03	1.69E-03	4.83E+00	1.35E-06	***
Age	1.05E-02	2.32E-03	4.55E+00	5.43E-06	***
Glue: present	-9.19E-01	2.14E-01	-4.30E+00	1.72E-05	***
Green Index	2.29E+00	6.06E-01	3.78E+00	1.54E-04	***
Leaf kg m ⁻²	1.30E+01	4.40E+00	2.97E+00	3.02E-03	***
Quality: medium	-5.38E-01	1.94E-01	-2.78E+00	5.45E-03	***
Quality: poor	-7.35E-01	2.93E-01	-2.51E+00	1.21E-02	**
Julian Day	4.38E-03	2.50E-03	1.75E+00	7.93E-02	.
Leaf stage: young	-2.85E-01	2.68E-01	-1.07E+00	2.87E-01	
Damage: medium	-1.26E+01	3.60E+02	-3.51E-02	9.72E-01	
Damage: minor	-1.25E+01	3.60E+02	-3.47E-02	9.72E-01	
Damage: none	-1.24E+01	3.60E+02	-3.44E-02	9.73E-01	

488



490

491 **Fig. 7:** Comparison of distributions of probabilities of assignment of each scan to a specific class for
 492 correctly (true-positive) or incorrectly classified (false-positive) specimens by leaf characteristics (see
 493 Table 1). A) Specimen quality observations primarily reflecting discoloration or tissue degradation. B)
 494 The presence or absence of mounting glue on the leaf. C) Visible biotic contamination, pre- or post-
 495 mortem damage to leaves. D) Leaf phenological development. Significant pairwise differences among
 496 correct or incorrect classes were determined using t-tests and indicated with the codes: * ($p < 0.05$), **
 497 ($p < 0.01$), and *** ($p < 0.001$). Note there were no significant differences among classification probabilities
 498 for incorrect predictions.



499

500 **Fig. 8:** Relationships between numeric predictor variables and classification outcomes. (A) Relationship
 501 between age (years) and classification probability, (B) relationship between green index and classification
 502 probability, (C) relationship between age (years) and green index, and (D) relationship between nearest
 503 taxon distance (NTD, M years) and classification probability. Points represent individual observations
 504 colored by correct versus incorrect status. Solid lines represent linear regression fits for each dataset.

505

506

507

508

509 Discussion

510 As the largest scientific repositories of plant diversity, herbaria offer exceptional resources for
511 investigations of plant biology, but their utility is shaped by the condition of preserved tissues. Recent
512 advances have proven the utility of spectra from pressed leaves (*i.e.* collected, pressed, dried, stored in
513 newspaper) on the order of months to years old for taxonomic classification (Durgante *et al.*, 2013; Lang
514 *et al.*, 2017; Kothari *et al.*, 2023) and functional trait estimation (Lang *et al.*, 2017; Kothari *et al.*, 2023).
515 Our study has extended this discovery to clearly demonstrate that herbarium specimens retain enough
516 morphological and anatomical integrity to be useful for the same spectra-based inferences.

517 The success of this proof-of-concept highlights the potential of reflectance spectroscopy as a
518 valuable addition to herbarium digitization pipelines (Hedrick *et al.*, 2020; Davis, 2023). To fully realize
519 this potential, the collections community must work collaboratively to establish standardized protocols
520 that ensure the compatibility of spectra collected across institutions (Fig. 2). Advancing standardized
521 protocols will require clear communication of the fundamental concepts of reflectance spectroscopy and
522 the myriad yet understudied factors influencing spectra from herbarium specimens. While our study has
523 identified many of these factors, much remains to be explored. Here, we aim to outline these
524 considerations and challenges as a foundation for the advancement of herbarium reflectance spectroscopy.

525 Considerations and challenges for herbarium reflectance spectroscopy

526 Biological variation

527 The goal of phenomic assessments is to characterize biological variation, but researchers must recognize
528 that spectral scans capture the cumulative effects of all factors—both natural and artifactual—that
529 influence reflected light. Before considering the effects of specimen processing and storage, researchers
530 should record metadata for developmental, phenological, and ecological factors that might influence leaf
531 structure and physiology.

532 For instance, herbarium specimens representing species with asynchronous flowering or fruiting
533 may disproportionately contain young, developing leaves or reproductive structures, leading to spectra
534 that do not adequately represent mature leaves (Fig. 2A). This variation introduces potential biases that
535 researchers should consider when interpreting spectral data. Alternatively, given the considerable changes
536 in leaf traits caused by phenology, traits will not be accurately estimated by models trained on one
537 phenological stage if the spectra were sampled from a different phenological stage. However, predictive
538 models show promise in accommodating such biological variation as long as models are trained to “see”
539 the full range of variation (Lang *et al.*, 2015).

540 In our study, mature leaves and young leaves were classified correctly the same proportion of
541 times because both of these traits were modeled (see Results). For traits, models should be trained from
542 datasets that span the range of trait values expected in testing datasets.

543 Additionally, tissue heterogeneity within a single leaf must be considered. Researchers should
544 avoid scanning leaf midribs, as their higher proportion of vascular tissue will influence spectra. Sampling
545 protocols should prioritize mature laminar leaf regions to ensure that spectral measurements accurately
546 reflect the traits of interest.

547 Herborization

548 The herborization process, which encompasses the preservation and storage of collected specimens,
549 presents a wide range of variables affecting plant tissues (Fig. 2A). During collection, plants are pressed
550 flat in newspaper shortly after collection, ideally before wilting. If drying cannot be performed within 24–
551 48 hours, specimens are typically soaked in 50–95% ethanol and sealed to prevent fungal growth.
552 Historically, other preservatives like formaldehyde have also been used. Drying methods vary, ranging
553 from forced-air systems or industrial ovens (30–70°C for 15–48 hours) to passive drying in arid
554 environments (Bridson *et al.*, 1998; Forrest *et al.*, 2019). Other analog methods necessary in more remote
555 locations, such as drying over hot coals, apply even hotter and more variable temperatures and are the
556 cause of the occasional encounter with a partially burnt specimen. Improperly dried specimens, on the
557 other hand, may exhibit discoloration, structural degradation, or fungal growth.

558 We assessed the impact of visual cues about the quality of herbarium specimens via our metadata
559 collection on specimen quality - our general interpretation of degradation as interpreted from
560 discoloration, wilting, pathogens, or signs of poor initial preservation - and on specimen damage. Medium
561 and poor herbarium quality classes were inferred to be significantly negatively correlated with correct
562 predictions (Table 4; Table S3), showing that apparent specimen degradation does indeed translate to
563 reduced model accuracy. The damage metadata was primarily used to annotate specimens with obvious
564 tissue alterations such as herbivory or burning that affected part of the specimen but usually not the
565 scanned leaves. Apart from the curious result of the six scans from two specimens of *Populus tremuloides*
566 with major damage having high classification probability yet low species classification accuracy (63%),
567 the more damaged leaves also followed expectations of reduced model performance. However, this was
568 not a significant factor in the logistic regression nor the random forest analysis.

569 After drying, specimens are transported, frozen for one to two weeks to eliminate insects, and
570 then mounted on herbarium sheets using glue, tape, or sewing. Herbarium sheets are typically made from
571 acid-free, lignin-free paper or cardboard, designed to prevent chemical reactions that could damage
572 specimens over time (Drobic, 2008). Acid-free paper resists yellowing and brittleness, as acidic

573 materials in the paper will otherwise degrade both the sheet and the plant material, altering the specimen's
574 color and structural integrity. However, not all herbaria have access to these archival-quality sheets. In
575 such cases, locally available paper may be acidic and will accelerate specimen degradation.

576 While sewing specimens to the herbarium sheets is the most durable and secure method, it is
577 highly labor-intensive and impractical for most herbaria with limited staff. Consequently, glues are the
578 most widely used adhesive in the United States. Many institutions rely on water-based glues such as
579 Elmer's® Glue-All or Jade 403® because they are easy to apply and generally effective. Glues are either
580 painted or sprayed onto the specimen's backside and blotted dry before pressing the specimen against the
581 sheet for adhesion. However, not all glues are ideal for long-term preservation. Some glues contain acidic
582 or unstable components that can break down over time, causing discoloration, loss of adhesion, or
583 chemical reactions that further degrade both the sheet and specimen. It is common to observe old glues or
584 stains from previous adhesives on older specimens that have been remounted through time. As such, there
585 are a variety of adhesives that have been used through the decades that need to be accounted for if
586 scanned, and furthermore, the leaves of some specimens may contain multiple layers of different
587 adhesives.

588 Due to their potential for direct contamination of spectra, glue is the most significant
589 contaminating source for herbarium spectra. Our study demonstrated a clear reduction in the probability
590 of correct classifications when glue is present on the leaf (Figure 7B) and significant impact of glue on
591 classification success (Table 4). We have tried and are aware of efforts to 'unmix' or 'subtract' the glue or
592 paper spectra from the leaf using different spectral libraries of these contaminants, but thus far we are not
593 aware of any solutions to isolate the leaf signal from a spectral profile that contains these extra materials.
594 As detailed below, it is critical to standardize scanning backgrounds to ensure protocol consistency and
595 data interoperability.

596 After mounting, labels containing collection data and envelopes or 'packets' for loose tissues are
597 attached to the sheets before specimens are stored in herbarium cabinets. Although large herbaria in the
598 global north often maintain temperature and humidity controls, daily, seasonal, and annual humidity
599 fluctuations remain a significant challenge worldwide, potentially accelerating specimen degradation.

600 Sampling herbarium specimens

601 When selecting specimens for sampling, researchers must choose among different herbarium specimens
602 and then among different leaves. The selected leaves should be mature and free from biotic pathogens or
603 contaminants (unless such factors are within the scope of the investigation), yet otherwise representative
604 of the normal variation in the specimen (Fig. 2A).

605 Our results on the age and greenness of the specimens might appear counterintuitive since these
606 two variables are, intuitively, negatively correlated; younger specimens tend to retain more greenness, and
607 green specimens are often assumed to represent better-preserved tissues. However, the relationship
608 between age and greenness, and their combined effect on methodological success, is more complex.
609 While DNA sequencing success – a methodology also reliant on tissue preservation – is frequently
610 assumed to decline with age, studies frequently show weak or no correlation between specimen age and
611 sequencing outcomes (Erkens *et al.*, 2008; Forrest *et al.*, 2019; White *et al.*, 2021). Instead, specimen
612 processing methods during the early stages of preservation appear to play a much more critical role in
613 tissue preservation.

614 Greenness, influenced by the presence of chlorophyll, has been shown to significantly affect
615 optical properties, particularly in the visible spectrum. While green tissues may indicate good
616 preservation, high chlorophyll concentrations in tissues can also mask other spectral features that might
617 be more informative for downstream applications like functional trait prediction or classification
618 modeling. The absence of chlorophyll, as seen in older or less green specimens, could enhance the
619 detection of structural and biochemical features that are less visible in green leaves (Kothari *et al.* 2023).
620 Thus, while greenness remains an important indicator of specimen preservation, its role in spectral data
621 acquisition and prediction success may depend on the specific objectives of the study.

622 Light transmitted through scanned leaves may reflect from the background (glue, paper, and even
623 lab benches), which ‘contaminates’ the spectrum, resulting in erroneously high measurements of leaf
624 reflectance. The degree of contamination depends on the optical thickness of the leaves, which governs
625 how much light is transmitted. Our analysis identified a significant positive correlation of LMA with
626 classification success, suggesting that thicker leaves that scatter more light perform better for prediction.
627 We believe it is critical that researchers avoid such contamination by scanning leaves against a black
628 background that absorbs nearly all transmitted light, which is currently being implemented through two
629 different protocols (Fig. 2B). First, if the specimen has been sewn or taped, it may be possible to slide a
630 thin black sheet between the attached leaf and the paper. Second, and preferable, herbarium specimens
631 with loose leaves available in packets may be selected and those leaves checked for glue before being
632 scanned in a leaf clip or against a black background.

633 Selection of these black backgrounds is a critical component of standardization that is just now
634 being evaluated experimentally. Researchers are currently using EVA foam and other black plastic
635 (Flavia Durgante, pers. comm.), black card stock painted with Krylon® Camouflage Matte Black spray
636 paint (Aaron Lee, pers. comm.), and SpectralBlack® foil (Samantha Bazan, Thomas Couvreur, pers.
637 comm), plus the black backgrounds of manufacturer leaf clips for portable spectroradiometers (Malvern

638 Panalytical, Spectral Vista Corporation, Spectral Evolution). The identification and adoption of a
639 universal background standard represents one of the most important objectives of protocol development.

640 Instrumentation

641 Beyond the tissues and backgrounds, instrumentation variables play a critical role in shaping spectral
642 profiles, adding complexity to the use of herbaria for spectral data collection (Fig. 2B). A standard
643 scanning protocol begins by allowing the instrument's light source to warm up and stabilize. During this
644 time, researchers should record appropriate metadata, including a standardized filename reflecting the
645 herbarium accession number. Once the instrument is ready, a white reference calibration standard is
646 scanned to establish 100% reflectance across wavelengths. Regularly calibrating the instrument with a
647 clean white reference standard for every specimen scanned ensures accuracy in reflectance calculations
648 from radiance. With the calibration complete, the instrument is ready to scan the sample leaf tissue placed
649 on a black background.

650 Additional factors influencing spectral data quality include the sensitivity of fiber optics, the
651 duration of scans, the geometry of the optical measurement setup (e.g. the angle of incidence) and the
652 potential for light sources to heat and alter leaf properties during scanning. These factors can also change
653 with leaf properties, such as highly rugose leaves or small, round leaves or needles. Variations in
654 fiberoptic alignment or quality can impact the signal-to-noise ratio, requiring careful handling and regular
655 replacement. Regular replacement of calibration standards and routine instrument maintenance, such as
656 cleaning and recalibrating sensors, are essential to sustaining instrument performance. Users select
657 integration time, during which instruments perform multiple rapid scans. Prolonged scanning times can
658 improve signal quality but may introduce heat effects on the specimen, which must be avoided.

659 Researchers may choose to process raw spectra with resampling and normalization or
660 transformation using derivatives or continuous wavelet transforms (CWT) to standardize datasets from
661 different instruments. We caution against band resampling at higher resolution than was measured by the
662 instrument as this could introduce artificial data to the spectrum. In our study, we used 5 nm resampling
663 for band spacing to harmonize the differences in spectral resolution between sensors (i.e., Spectral
664 Evolution PSR+ and SVC HR-1024i) and reduce the number of correlated bands for predicting models.
665 The raw, 1.4 nm bandwidths did return a higher overall accuracy of taxonomic classification.

666 Researchers will also typically trim the 350–400 nm and 2,400–2,500 nm regions because they
667 might have a lot of noise. Additionally, we further trimmed our data in later stages of analysis after
668 noticing reflectance and VIP differences between herbarium datasets between the pressed and in the 400-
669 450 nm range. However, the raw spectral data should be archived so future users can choose and improve
670 upon data preprocessing steps.

671 The success of data aggregation for herbarium spectral scans depends on the adoption of
672 standardized protocols. To this end, we are actively collaborating with individuals from diverse
673 institutions to establish robust and universally applicable methodologies for herbarium spectroscopy.
674 These efforts aim to ensure consistency and reproducibility across studies, paving the way for expanded
675 applications in plant biology and global ecology.

676 Data aggregation

677 The success of herbarium reflectance spectroscopy hinges on robust data aggregation practices that ensure
678 consistency, interoperability, and accessibility across institutions (Fig. 2C). Metadata standardization is
679 critical for harmonizing datasets, as it facilitates the integration of phenomic data with associated
680 specimen metadata, such as taxonomy, collection locality, and ecological context. By adopting common
681 metadata schemas and persistent identifiers (DOIs), researchers can link spectral data directly to digital
682 databases, fostering seamless collaboration and data reuse. Experience gained from successful protocol
683 standardization and data aggregation initiatives (e.g. Darwin Core and iDigBio; Wieczorek *et al.*, 2012;
684 Soltis, 2017) can be leveraged to implement a strategy for herbarium spectroscopic data.

685 The development of cyberinfrastructure has been pivotal in enabling large-scale aggregation of
686 spectral data. Platforms like iDigBio and GBIF provide centralized repositories for biodiversity data, but
687 dedicated cyberinfrastructure for spectral datasets, integrated with existing platforms, will be essential for
688 advancing collections-based research. These systems should support real-time synchronization of
689 available data from herbarium institutions, cross-referencing, and retrieval for global accessibility. Any
690 dedicated spectral cyberinfrastructure platforms will require Application Programming Interfaces (APIs)
691 to enable researchers to query, retrieve, and contribute spectral datasets programmatically; facilitating the
692 large-scale synthesis of data. Existing cyberinfrastructure developed specifically for spectral data and
693 models, such as EcoSis and EcoSML (Wagner *et al.*, 2019), can be leveraged for herbarium data or used
694 as models for developing new infrastructure.

695 Ensuring data quality controls is another foundational aspect of data aggregation. These controls
696 include rigorous preprocessing of spectral datasets (e.g., noise removal, calibration) and standardization
697 of scanning protocols to maintain the highest possible consistency across instruments, collections, and
698 institutions. Routine validation processes will ensure that aggregated data meet the necessary standards
699 for reproducibility and analysis. Finally, the implementation of analysis engines capable of handling high-
700 dimensional datasets will be transformative. These engines should integrate spectral data with
701 complementary datasets, such as genomic or spatial data, and provide tools for advanced modeling and
702 visualization. Open-source analysis platforms with user-friendly interfaces will democratize access to
703 these tools and foster collaboration across disciplines.

704 Scaling herbarium reflectance spectroscopy

705 As we consider the broader utility of herbarium specimens for estimating traits, the successful transfer of
706 pressed-leaf models onto herbarium spectra offers a powerful method for reconstructing traits as they
707 would have existed in vivo. This approach not only enhances the ecological relevance of trait predictions
708 from herbarium specimens but also circumvents the need for destructive sampling of these invaluable
709 collections. By preserving specimen integrity, reflectance spectroscopy provides a non-destructive,
710 scalable, and integrative methodology for linking historical plant traits to modern ecological and
711 evolutionary studies (Costa *et al.* 2018; Kothari *et al.* 2023).

712 Advancing collections-based spectroscopy for plant biology and global ecology is increasingly
713 critical, particularly given the current vulnerabilities faced by herbaria and collection facilities. Despite
714 their pivotal role in biodiversity research, herbaria often face devaluation and threats of closure (Thiers,
715 2024; Davis, 2024). At the same time, advances in digital technologies and biological data networks are
716 unlocking unprecedented opportunities for their use (Meineke *et al.*, 2018; Lang *et al.*, 2019; Hedrick *et*
717 *al.*, 2020; Bakker *et al.*, 2020; Heberling, 2022; Davis, 2023). Over the past fifteen years, targeted funding
718 initiatives, such as those supported by the U.S. National Science Foundation, have facilitated the creation
719 of comprehensive digital databases containing specimen images, metadata, and extended datasets like
720 DNA sequences (Soltis, 2017). Platforms like iDigBio and GBIF now aggregate these resources into a
721 global "Metaherbarium"—an integrated digital repository of plant diversity and distributions (Davis,
722 2023). This Metaherbarium is already driving transformative, global-scale research in biodiversity,
723 ecology, and evolution, offering fresh insights into how plant life responds to environmental change
724 (Meineke *et al.*, 2018; Davis, 2023).

725 As the momentum for leveraging collections continues to grow, the balance between innovative
726 use and long-term preservation becomes increasingly vital (Davis *et al.*, 2024). The non-destructive
727 nature of reflectance spectroscopy aligns perfectly with this goal. Spectral data files can be seamlessly
728 integrated into digital specimen databases through persistent identifiers, linking these phenomic datasets
729 directly to physical specimens and their associated metadata. By avoiding physical alteration, reflectance
730 spectroscopy ensures the continued preservation of herbarium specimens for future research.

731 While functional trait prediction and taxonomic classification remain the most well-established
732 applications of spectral reflectance, the future promises exciting new integrations with complementary
733 datasets. In particular, the merging of spectral libraries with genomic, phenotypic, and spatial datasets
734 offers unprecedented opportunities for addressing ecological and evolutionary questions. For example,
735 these integrated datasets could facilitate species delimitation or provide novel insights into community
736 assembly and functional biogeography. The combination of spectral reflectance libraries with "omics"
737 and other synthetic datasets holds tremendous potential for generating new inferences about plant

738 diversity, distributions, and functional traits across temporal and spatial scales (Cavender-Bares *et al.*,
739 2017; Davis, 2023). Such advancements will continue to transform biodiversity science, bridging
740 historical collections with cutting-edge methodologies to address the pressing ecological and evolutionary
741 questions of our time.

742 **References:**

743

744 **Abasolo M, Lee DJ, Raymond C, Meder R, Shepherd M. 2013.** Deviant near-infrared spectra
745 identifies *Corymbia* hybrids. *Forest Ecology and Management* **304**: 121–131.

746 **Bakker FT, Bieker VC, Martin MD. 2020.** Herbarium Collection-Based Plant Evolutionary Genetics
747 and Genomics. *Frontiers in Ecology and Evolution* **8**.

748 **Bieker VC, Sánchez Barreiro F, Rasmussen JA, Brunier M, Wales N, Martin MD. 2020.**
749 Metagenomic analysis of historical herbarium specimens reveals a postmortem microbial community.
750 *Molecular Ecology Resources* **20**: 1206–1219.

751 **Breiman L, Cutler A, Liaw A, Wiener M. 2024.** randomForest: Breiman and Cutlers Random Forests
752 for Classification and Regression.

753 **Bridson DM, Forman L, Royal Botanic Gardens K. 1998.** *The herbarium handbook*. Richmond,
754 Surrey: Royal Botanic Gardens, Kew.

755 **Cavender-Bares J, Gamon JA, Hobbie SE, Madritch MD, Meireles JE, Schweiger AK, Townsend**
756 **PA. 2017.** Harnessing plant spectra to integrate the biodiversity sciences across biological and spatial
757 scales. *American Journal of Botany* **104**: 966–969.

758 **Cavender-Bares J, Meireles JE, Couture JJ, Kaproth MA, Kingdon CC, Singh A, Serbin SP,**
759 **Center A, Zuniga E, Pilz G, et al. 2016.** Associations of leaf spectra with genetic and phylogenetic
760 variation in oaks: Prospects for remote detection of biodiversity. *Remote Sensing* **8**: 17–17.

761 **Cavender-Bares J, Meireles JE, Pinto-Ledezma J, Reich PB, Schuman M, Townsend PA,**
762 **Trowbridge A. In Review.** Spectral biology across scales in changing environments. *Ecology*.

763 **Chamberlain S, Oldoni D, Barve V, Desmet P, Geffert L, Mcglinn D, Ram K, Waller J. 2024.** rgbif:
764 Interface to the Global Biodiversity Information Facility API.

765 **Costa FRC, Lang C, Almeida DRA, Castilho CV, Poorter L. 2018.** Near-infrared spectrometry allows
766 fast and extensive predictions of functional traits from dry leaves and branches. *Ecological Applications*
767 **28**: 1157–1167.

768 **Cotrozzi L, Couture JJ, Cavender-Bares J, Kingdon CC, Fallon B, Pilz G, Pellegrini E, Nali C,**
769 **Townsend PA. 2017.** Using foliar spectral properties to assess the effects of drought on plant water
770 potential. *Tree Physiology* **37**: 1582–1591.

771 **Curran PJ. 1989.** Remote sensing of foliar chemistry. *Remote Sensing of Environment* **30**: 271–278.

772 **Davis CC. 2023.** The herbarium of the future. *Trends in Ecology & Evolution* **38**: 412–423.

773 **Davis CC. 2024.** Collections are truly priceless. *Science* **383**: 1035–1035.

774 **Davis CC, Sessa E, Paton A, Antonelli A, Teisher JK. 2024.** Guidelines for the effective and ethical
775 sampling of herbaria. *Nature Ecology & Evolution*: 1–8.

776 **Díaz S, Kattge J, Cornelissen JHC, Wright IJ, Lavorel S, Dray S, Reu B, Kleyer M, Wirth C, Colin**
777 **Prentice I, et al. 2016.** The global spectrum of plant form and function. *Nature* **529**: 167–171.

778 **Drobnic J. 2008.** Modern techniques of herbarium protection. *Scripta Facultatis Rerum Naturalium*
779 *Universitatis Ostraviensis* **186**.

780 **Durgante FM, Higuchi N, Almeida A, Vicentini A. 2013.** Species Spectral Signature: Discriminating
781 closely related plant species in the Amazon with Near-Infrared Leaf-Spectroscopy. *Forest Ecology and*
782 *Management* **291**: 240–248.

783 **Erkens RHJ, Cross H, Maas JW, Hoenselaar K, Chatrou LW. 2008.** Assessment of age and

784 greenness of herbarium specimens as predictors for successful extraction and amplification of DNA.
785 *Blumea - Biodiversity, Evolution and Biogeography of Plants* **53**: 407–428.

786 **Forrest LL, Hart ML, Hughes M, Wilson HP, Chung K-F, Tseng Y-H, Kidner CA. 2019.** The limits
787 of Hyb-Seq for herbarium specimens: Impact of preservation techniques. *Frontiers in Ecology and*
788 *Evolution* **7**.

789 **Fourty Th, Baret F, Jacquemoud S, Schmuck G, Verdebout J. 1996.** Leaf optical properties with
790 explicit description of its biochemical composition: Direct and inverse problems. *Remote Sensing of*
791 *Environment* **56**: 104–117.

792 **Funk JL, Larson JE, Ames GM, Butterfield BJ, Cavender-Bares J, Firn J, Laughlin DC, Sutton-**
793 **Grier AE, Williams L, Wright J. 2017.** Revisiting the Holy Grail: using plant functional traits to
794 understand ecological processes. *Biological Reviews* **92**: 1156–1173.

795 **GBIF.org.** GBIF Home Page. <http://www.gbif.org/>

796 **Guzmán Q. JA. 2024.** CWT: Continuous Wavelet Transformation for Spectroscopy.

797 **Guzmán Q. JA, Sanchez-Azofeifa GA. 2021.** Prediction of leaf traits of lianas and trees via the
798 integration of wavelet spectra in the visible-near infrared and thermal infrared domains. *Remote Sensing*
799 *of Environment* **259**: 112406.

800 **Heberling JM. 2022.** Herbaria as Big Data Sources of Plant Traits. *International Journal of Plant*
801 *Sciences* **183**: 87–118.

802 **Hedrick BP, Heberling JM, Meineke EK, Turner KG, Grassa CJ, Park DS, Kennedy J, Clarke JA,**
803 **Cook JA, Blackburn DC, et al.2020.** Digitization and the Future of Natural History Collections.
804 *BioScience* **70**: 243–251.

805 **Jetz W, Cavender-Bares J, Pavlick R, Schimel D, Davis FW, Asner GP, Guralnick R, Kattge J,**
806 **Latimer AM, Moorcroft P, et al.2016.** Monitoring plant functional diversity from space. *Nature Plants*
807 **2**: 1–5.

808 **Jin Y, Qian H. 2022.** V.PhyloMaker2: An updated and enlarged R package that can generate very large
809 phylogenies for vascular plants. *Plant Diversity* **44**: 335–339.

810 **Kothari S, Beauchamp-Rioux R, Laliberté E, Cavender-Bares J. 2023.** Reflectance spectroscopy
811 allows rapid, accurate and non-destructive estimates of functional traits from pressed leaves. *Methods in*
812 *Ecology and Evolution* **14**: 385–401.

813 **Kothari S, Schweiger AK. 2022.** Plant spectra as integrative measures of plant phenotypes. *Journal of*
814 *Ecology* **110**: 2536–2554.

815 **Kuhn M, Wing J, Weston S, Williams A, Keefer C, Engelhardt A, Cooper T, Mayer Z, Kenkel B, R**
816 **Core Team, et al.2024.** caret: Classification and Regression Training.

817 **Kumar S, Suleski M, Craig JM, Kasprovicz AE, Sanderford M, Li M, Stecher G, Hedges SB. 2022.**
818 TimeTree 5: An Expanded Resource for Species Divergence Times. *Molecular Biology and Evolution* **39**:
819 msac174.

820 **Lang C, Almeida DRA, Costa FRC. 2017.** Discrimination of taxonomic identity at species, genus and
821 family levels using Fourier Transformed Near-Infrared Spectroscopy (FT-NIR). *Forest Ecology and*
822 *Management* **406**: 219–227.

823 **Lang C, Costa FRC, Camargo JLC, Durgante FM, Vicentini A. 2015.** Near infrared spectroscopy
824 facilitates rapid identification of both young and mature Amazonian tree species. *PLoS ONE* **10**:
825 e0134521–e0134521.

826 **Lang PLM, Willems FM, Scheepens JF, Burbano HA, Bossdorf O. 2019.** Using herbaria to study

827 global environmental change. *New Phytologist* **221**: 110–122.

828 **Liland KH, Mehmood T, Sæbø S. 2024a.** plsVarSel: Variable Selection in Partial Least Squares.

829 **Liland KH, Mevik B-H, Wehrens R, Hiemstra P. 2024b.** pls: Partial Least Squares and Principal
830 Component Regression.

831 **Meineke EK, Davis CC, Davies TJ. 2018.** The unrealized potential of herbaria for global change
832 biology. *Ecological Monographs* **88**: 505–525.

833 **Meireles JE, Cavender-Bares J, Townsend PA, Ustin S, Gamon JA, Schweiger AK, Schaepman
834 ME, Asner GP, Martin RE, Singh A. 2020.** Leaf reflectance spectra capture the evolutionary history of
835 seed plants. *New Phytologist* **228**: 485–493.

836 **Meireles JE, Schweiger A, Cavender-Bares J. 2017.** Spectrolab: class and methods for hyperspectral
837 data. *R package version 0.0 2*.

838 **Neto-Bradley BM, Bonnet P, Goeau H, Joly A, Cavender-Bares J, Coomes DA.** Using reflectance
839 spectra and Pl@ntNet to identify herbarium specimens: a case study with *Lithocarpus*. *New Phytologist*.

840 **R Core Team. 2023.** *R: A Language and Environment for Statistical Computing*. Vienna, Austria: R
841 Foundation for Statistical Computing.

842 **Serbin SP, Singh A, McNeil BE, Kingdon CC, Townsend PA. 2014.** Spectroscopic determination of
843 leaf morphological and biochemical traits for northern temperate and boreal tree species. *Ecological
844 Applications* **24**: 1651–1669.

845 **Serbin SP, Townsend PA. 2020.** Scaling Functional Traits from Leaves to Canopies. In: Cavender-Bares
846 J, Gamon JA, Townsend PA, eds. *Remote Sensing of Plant Biodiversity*. Cham: Springer International
847 Publishing, 43–82.

848 **Soltis PS. 2017.** Digitization of herbaria enables novel research. *American Journal of Botany* **104**: 1281–
849 1284.

850 **Stasinski L, White DM, Nelson PR, Ree RH, Meireles JE. 2021.** Reading light: leaf spectra capture
851 fine-scale diversity of closely related, hybridizing arctic shrubs. *New Phytologist* **232**: 2283–2294.

852 **Thiers B. 2020.** Index Herbariorum: A worldwide index of 3,100 herbaria and 12,000 associated staff
853 where a total of 390 million botanical specimens are permanently housed.

854 **Thiers BM. 2024.** Strengthening Partnerships to Safeguard the Future of Herbaria. *Diversity* **16**: 36.

855 **Wagner EP, Merz J, Townsend PA. 2019.** EcoSIS: A Spectral Library and the Tools to Use It. **2019**:
856 B11F-2396.

857 **White DM, Huang J-P, Jara-Munoz OA, Madriñán S, Ree RH, Mason-Gamer RJ. 2021.** The
858 Origins of Coca: Museum Genomics Reveals Multiple Independent Domestications from Progenitor
859 *Erythroxylum gracilipes*. *Systematic Biology* **70**: 1–13.

860 **Wickham H, Chang W, Henry L, Pedersen TL, Takahashi K, Wilke C, Woo K, Yutani H,
861 Dunnington D, Brand T van den, et al. 2024.** ggplot2: Create Elegant Data Visualisations Using the
862 Grammar of Graphics.

863 **Wieczorek J, Bloom D, Guralnick R, Blum S, Döring M, Giovanni R, Robertson T, Vieglais D.
864 2012.** Darwin Core: An Evolving Community-Developed Biodiversity Data Standard. *PLOS ONE* **7**:
865 e29715.

866 **Wright IJ, Reich PB, Westoby M, Ackerly DD, Baruch Z, Bongers F, Cavender-Bares J, Chapin T,
867 Cornelissen JHC, Diemer M, et al. 2004.** The worldwide leaf economics spectrum. *Nature* **428**: 821–
868 827.

869

870

871

872 Acknowledgements

873 We thank the curatorial and digitization staff at the Harvard University Herbaria (HUH) for past and
874 present efforts to curate and digitize the Herbaria, with special thanks to Michaela Schnull and Lisa
875 Standley for support and protocol development. Nico Gascon and Sydney Kaye assisted with specimen
876 imagery. This project was funded by the NSF BII DBI-2021898 (JCB and JEM), the Harvard University
877 Herbaria Postdoctoral Research Fellowship (DMW), and an NSF REU award 2150058 (JMR).

878

879 Author Contributions

880 JC-B, CCD, JAGQ, SK, JEM, and DMW conceptualized the project. JC-B, JAGQ, JEM, and DMW
881 developed the methodology. JAGQ, JMR, and DMW curated the data. JMR and DMW conducted the
882 investigation. DMW performed the formal analysis. JC-B and DMW secured funding and managed the
883 project. JC-B and SK provided resources. JAGQ, JEM, and DMW developed the software. JC-B, JEM,
884 and DMW supervised the project. JAGQ and DMW validated the results. JAGQ, JEM, and DMW created
885 visualizations. JEM and DMW wrote the original draft and all authors reviewed and edited the final
886 version of the manuscript.

887

888 Data Availability Statement

889 All analysis codes used in this study are publicly available at GitHub
890 ([github.org/Erythroxyllum/herbarium-spectra](https://github.com/Erythroxyllum/herbarium-spectra)). Spectral data have been deposited in the EcoSIS repository
891 and can be accessed at <https://ecosis.org/>.